Yared Bekele • Anatoly O. Sinitsyn

Impact of Climate Change on Infrastructure in Longyearbyen

CASE STUDY OF PILE FOUNDATIONS ON SLOPING TERRAINS

SINTEF

SINTEF Notes

Yared Bekele and Anatoly O. Sinitsyn

Impact of Climate Change on Infrastructure in Longyearbyen

Case Study of Pile Foundations on Sloping Terrains

SINTEF Academic Press

Foreword

This report presents findings from studies in the project entitled "*Impact of Changing Climate on Infrastructure in Longyearbyen: Stability of Foundations on Slope Terrain – Case Study*" carried out at SINTEF. The financial support for the project was obtained from Svalbards Miljøvernfond, Longyearbyen Lokalstyre and Store Norske Spitsbergen Kulkompani AS. Climate data used in this study was provided by The Norwegian Meteorological Institute. The project was initiated through a proposal submitted to the Svalbard Miljøvernfond in the fall of 2016. The initiative targeted planning in Longyearbyen under conditions of climate change.

The main purpose of the project was to perform studies on how climate change affects infrastructure foundations on slope terrain in permafrost. The study was performed with the aim of maintaining the functionality of existing buildings and to provide valuable engineering knowledge for the proper consideration of climate change in the design of new infrastructure in Longyearbyen.

Trondheim, 15.04.2020

Lisbeth-Ingrid Alnæs
Research Manager
SINTEF Community

Anatoly O. Sinitsyn
Project Leader
SINTEF Community

SVALBARD ENVIRONMENTAL
PROTECTION FUND

Executive Summary

The effect of climate change on existing infrastructure in Longyearbyen, Svalbard is investigated in this study. Climate data recordings show that, over the past couple of years, record-breaking temperature and precipitations measurements are observed in this area. It is anticipated that this will pose a serious threat to existing infrastructure and will impose additional challenges for new developments. Adaptations of existing and future infrastructure to changes in climate for safety and serviceability is of paramount importance. The current study aims to contribute towards this initiative.

The particular focus of the study was slopes and buildings supported on sloping terrains in Longyearbyen. Changes in ground temperature are investigated based on existing temperature data and forecasts. The ground thermal regime is then used to evaluate the stability of representative slopes in the study area. The capacity of single piles on a slope is also investigated by considering various factors such as slope angle, location of pile on slope, pile material and geometry. The following findings are observed from the investigation:

The projected climate data show that temperatures will keep rising in Svalbard. Based on the analytical and numerical studies performed for the projected temperature data, it is observed that the active layer thickness will increase up to 2 m or more, depending on the thermal properties of the soil. The increase in ground temperatures also results in the warming of the permafrost underneath the active layer. The stability of slopes and the bearing capacity of existing infrastructure foundations is expected to be significantly affected by these changes.

Slope stability evaluations were performed for a representative slope in the study area by considering changing active layer thicknesses according to the projected ground temperature regime. The factor of safety against slope failure decreases with increasing active layer thickness. Under the specific assumptions made for the evaluation, the representative slope was found to be stable for active layer thicknesses of up to 2m. Sensitivity analyses show that the factor of safety is significantly affected by changes is material parameters such as cohesion and friction angle, which are associated with the ground thermal regime. Accurate estimation of material properties is required for a definitive slope stability evaluation.

The performance of single piles on a slope is investigated by performing various analytical and numerical studies. One of the effects of an increase in active layer thickness on sloping terrains is the risk of solifluction, which is a slow downward movement of soil. The soil movement exerts additional lateral forces on pile foundations, affecting the ultimate capacity of the piles. This is especially significant for building where the effect of solifluction is not considered in the original design. It is observed from the analyses that piles subjected to such additional lateral forces will experience increased deflections and internal forces. The deflections and internal forces increase with increasing slope angles and active layer thicknesses. Piles located in the middle of the slope are observed to experience larger deflections and internal forces than piles located at the toe of the slope. The effect of such increased deflections and internal forces is especially critical for timber piles where the capacity is expected (and shown) to reduce with aging.

Based on the observation from the current study, specific case study for a selected location was performed. The effects of increased lateral loads, as a result of thawing and warming permafrost, on the pile foundations of a selected building in Longyearbyen located on a slope are investigated through numerical analyses. A range of active layer thicknesses are considered in the analyses taking current and projected scenarios into account. The axial loads on the piles are estimated based on standard methods for residential buildings, and variations are considered to account for uncertainties. The lateral loads on the piles are assumed to mainly originate from slope movements (such as solifluction) and loads transferred from crest of the slope through earth pressure. The finite element simulations performed in a general way are

used a basis to estimate the earth pressures on the piles and the loads are converted to an equivalent resultant system at the pile head for simplicity of the analyses. Variations in the lateral loads are considered corresponding to the range of active layer thicknesses. Analyses based on p-y curves are performed for the different active layer thicknesses and loads considered. The results are presented in terms of pile head deflections, bending moments and shear forces. It is shown that the pile head deflections are expected to increase as the active layer thicknesses increase. A similar trend of increase is observed in the internal forces generated in the piles.

In general, the study here highlights the importance of assessing the effect of climate change on existing infrastructure to ensure safety and serviceability. The knowledge gained from the study also highlights the necessity of the consideration of climate change in the design of new infrastructure to be built in affected areas.

Contents

1 Introduction

1.1 Background

The last years exhibit record-breaking values of air temperatures and amount of precipitation in Svalbard. Several severe events caused by environmental hazards took place in Longyearbyen in the last decade and the last few years in particular. One may relate such events as manifestation of a changing climate.

It is believed that global climate warming will impose serious impact on infrastructure in the arctic. Assessment of impact of changing climate on arctic infrastructures was performed in [1]. Authors of the latter assessment point out increased concerns related to the impact of projected climate change on arctic infrastructure. In particular, projected climate change may "increase the environmental stresses structures are exposed to; affect geohazards and the impacts of extreme events."

Svalbard Archipelago has experienced warming during 20th century, especially in the last three decades [2]. Evaluations of future climate suggest significant air warming, increase of precipitation, and increasing storm frequency [3-5]. The latest observations at Svalbard airport show air temperatures and precipitations at values of much higher than normal. Moreover, July 2016 was the single warmest month ever recorded; [6].

Increase in air temperatures leads to degradation of permafrost. Consequences of permafrost degradation according to [7] consist in increased thickness of the active layer, warming of permafrost at depth, and permafrost thawing. One can expect that the latter phenomena will lead to decrease of bearing capacity of foundations based on permafrost. Assessment performed by [8] showed that theoretical pile capacity in Longyearbyen decreased insufficiently (by 12.5%) in the period 1977–2007. However, it is relevant to assess how existing foundations in Longyearbyen will withstand to projected climate change.

Increased intensity of rainfall may increase the risk for landslides in ice-rich permafrost [9], which may be facilitated by increase of thawing depths of the ground due to increased summer air temperatures. Solifluction, i.e. slow (with rates of few cm/yr) downslope flow of saturated unfrozen earth materials (in summertime, when the upper layer of permafrost is thawed), affects serviceability of foundations in Longyearbyen. Action of solifluction was not taken into account for the design of foundations for many buildings in Longyearbyen, [10]. Several issues related to solifluction can be observed today. An important question to be answered is "Will existing infrastructure on slope terrain hold up in new conditions taking place due to climate change?"

1.2 Description of the Initiative

The initiative suggests performing an assessment of vulnerability of selected infrastructures in Longyearbyen due to projected changes in climate. It is suggested to perform an assessment of bearing capacity and serviceability analysis of pile foundations (taking solifluction into account) of existing buildings on slope terrain.

The assessment is needed for managing the existing buildings and for future areal planning. The following particular reasons are also considered:

- Significant number of buildings in slope terrain in Longyearbyen are experiencing issues due to slope processes (solifluction). Therefore, an assessment is needed in order to foresee when and what kind of interaction has to be done in order maintain functionality of existing buildings.

- The areas with slope terrain should not be excluded from the planning of residential buildings and other infrastructures, but foundation solutions shall be obtained to fulfil requirements of serviceability (requirements to acceptable settlements and displacements).

1.3 Infrastructure for the Study

Initially suggested area [11] and several buildings and slope areas identified as suitable for the research [12] are presented on Figure 1.

Figure 1: Buildings and areas identified for the current study. Map: [34].

Building at Vei 232.16 and area up slope was selected by the participants of the kick-off meeting as preferable study object within the project. This slope may be considered to be in "isolated solifluction conditions", i.e. on minimal artificial changes (cut profiles or berms) are introduced into this slope.

Field work was conducted at the preferable study area in early March 2017.

2   Ground Thermal Regime

The ground thermal regime is investigated based on existing temperature data and forecasts. The air temperature data is used to calculate the progression in the air thawing index and the active layer thickness. Analytical calculations and numerical simulations are performed to study the expected evolution of ground temperatures based on the temperature forecasts. The ground temperature calculated here will serve as an input for the calculation of the bearing capacity of pile foundations in later sections.

2.1   Longyearbyen Air Temperatures

The air temperature data for Longyearbyen based on existing data and forecasts is presented here. Parameters relevant for studying ground thermal regimes are determined based on these data.

2.1.1   Existing Data and Forecast

Air temperature data and forecasts for Longyearbyen are obtained from The Norwegian Meteorological Institute through personal communications with Rasmus E. Benestad. Climate projections for Svalbard are courtesy of The Norwegian Meteorological Institute and other collaborators are reported in publications such as [4] and [5].
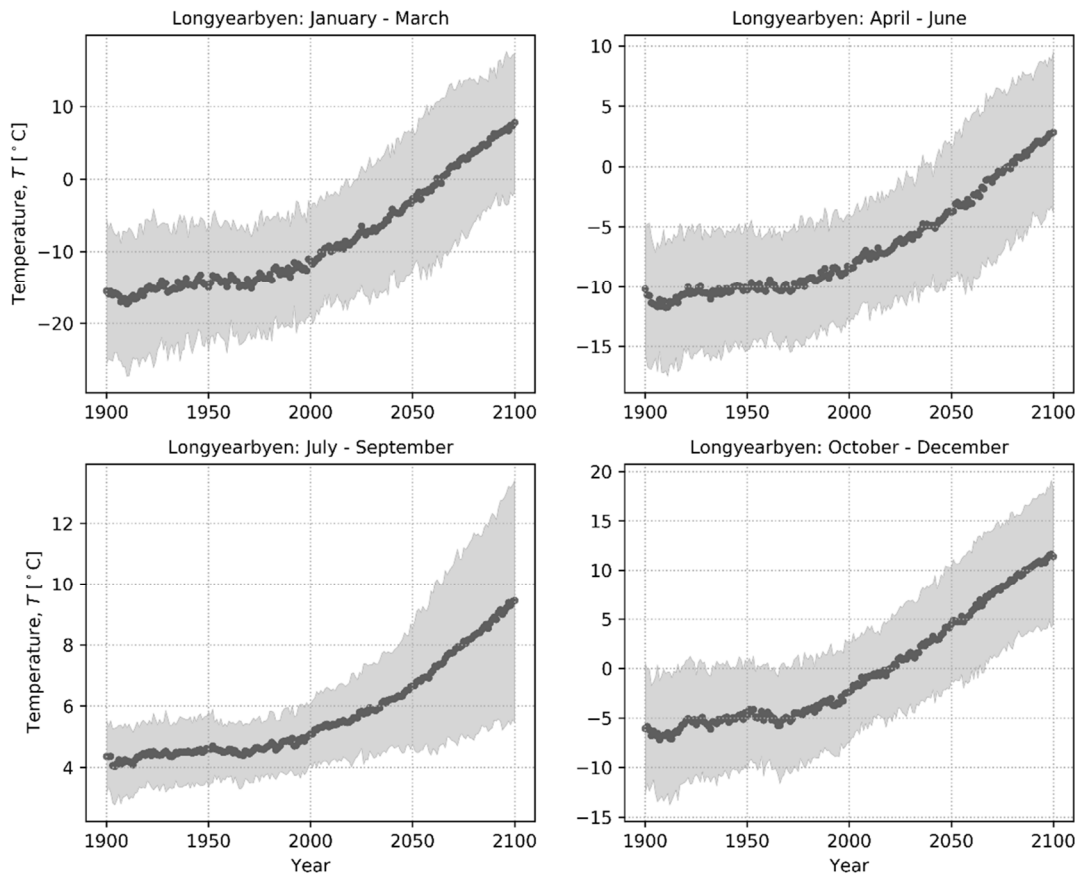
Figure 2: Longyearbyen air temperature progression from existing data and downscaled forecast in terms of seasonal mean values. The forecast is corresponding to RCP8.5. Data courtesy of Rasmus E. Benestad, The Norwegian Meteorological Institute.

The downscaled seasonal mean temperatures for Longyearbyen based on RCP8.5 are presented and used here. RCP8.5 is the scenario with highest greenhouse gas concentrations, which provides the highest projecting of global warming increase. The seasonal mean

temperatures and standard deviations are obtained and these are believed to provide more robust estimates as the mean is better estimated for a seasonal sample than for a monthly or daily sample. The seasonal means and standard deviations can be used to predict daily temperatures whenever necessary, as will be discussed in subsequent sections.

The air temperature data and forecast are available for the period from $1900 - 2100$. The upper and lower bounds are estimated assuming a normal distribution for the temperature; see for example [4]. The evolution of the seasonal mean temperature, including the estimated upper and lower bounds, are shown in Figure 2.

2.1.2 Air Freezing and Thawing Indices

The air thawing and freezing indices are defined as the aggregate durations (usually reported in number of days) when the air temperatures are below and above the freezing temperature; see [13]. The air freezing index (I_{af}) is an important parameter for the estimation of the maximum depth of ground-frost penetration depth. The air thawing index (I_{at}) is used for the prediction of permafrost distribution and for the estimation of thaw depth in frozen ground.
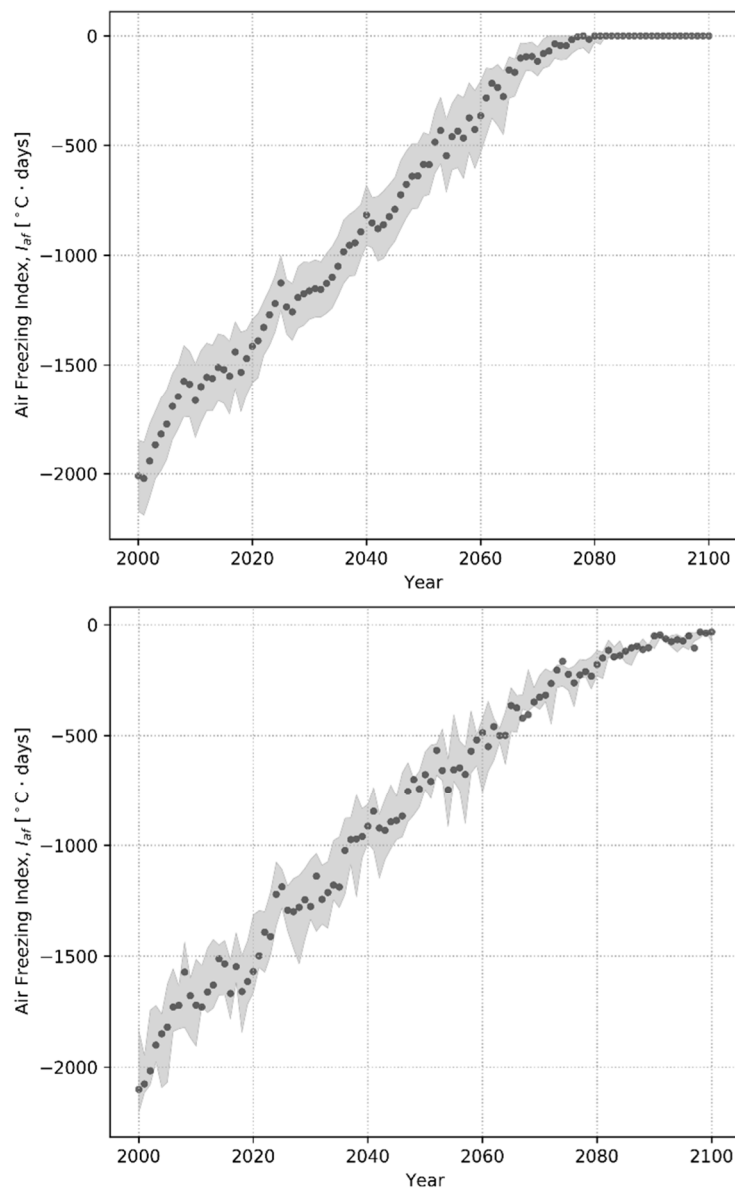

Figure 3: Air freezing indices based on seasonal mean temperatures (top) and inferred daily temperatures (bottom).

The air freezing and thawing indices are calculated based on the temperature data and forecast presented in Figure 2. The air freezing indices based on seasonal means and inferred daily temperatures are shown in Figure 3. It can be seen from the figure that all seasonal mean temperatures beyond ca. 2080 are all positive. Similarly, the air thawing indices based on seasonal mean and inferred daily temperatures are shown in Figure 4. The daily temperatures are inferred from the seasonal means and standard deviations by assuming a normal distribution. Both results are shown for the year periods from 2000 – 2100.
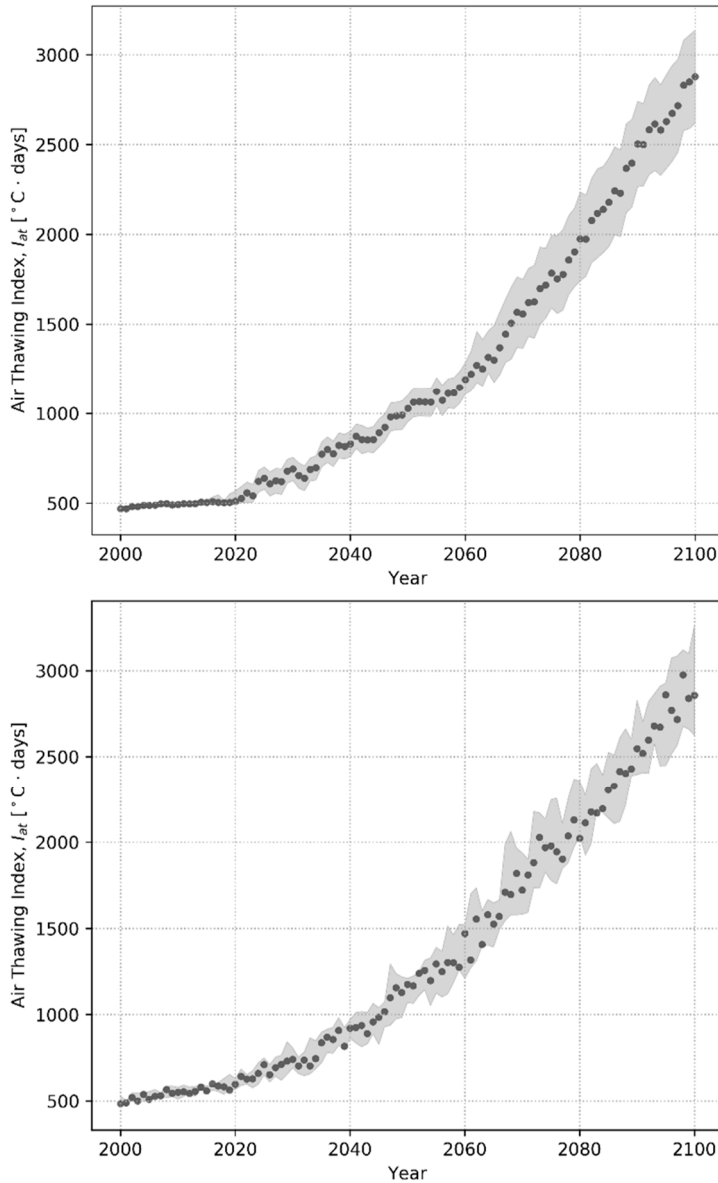

Figure 4: Air thawing indices based on seasonal mean temperatures (top) and inferred daily temperatures (bottom).

2.2   Active Layer: Analytical Calculations

The active layer is the soil above permafrost that freezes and thaws seasonally. The thickness of the active layer is governed by soil temperature which is a product of heat exchange between the atmosphere (air temperature) and ground surface; [14]. The thickness of the active layer is affected by several factors. Some of the broader factors include solar isolation patterns, latitude of the location, elevation of the area and proximity to glaciers and water bodies. Local factors that govern the active layer thickness include amount of snow cover (which depends on amount of precipitation, temperature, wind patterns, ground surface morphology), vegetation cover and soil type.

There are a number of analytical approaches which can be used to calculate the thickness of the active layer during seasonal freezing and thawing. Some of these analytical methods include the Modified Berggren Equation, the Neumann Equation and the Stefan Solution. We apply the Stefan Solution here to estimate the active layer thicknesses.

The details of the Stefan Solution can be referred from [13]. It is assumed in this method that the temperature distribution in the thawed soil is linear while the temperature in the frozen zone is ignored. In addition, the soil properties in the frozen and thawed zones are assumed to be homogeneous and independent of temperature. It is also assumed that the latent heat is liberated at 0°C in the thawing soil. Based on these assumptions, the thawing depth z_{th} for a frozen soil mass subjected to a step increase in temperature at the surface can be calculated from the expression

$$z_{th} = \sqrt{\frac{2\lambda_u T_s t}{L}} \tag{2.1}$$

where λ_u is the unfrozen soil thermal conductivity, T_s is the applied constant surface temperature, t is time and L is the volumetric latent heat of the soil. The applied constant surface temperature can be obtained from

$$T_s = \frac{I_{st}}{t} \tag{2.2}$$

where I_{st} is the ground surface thaw index expressed as a function of the air thawing index I_{at} as

$$I_{st} = n_t I_{at} \tag{2.3}$$

where n_t is called the thawing n-factor. This factor is used to consider the difference between air temperatures and ground surface temperatures as this have been shown to be different. The magnitude of n_t depends on several factors such as net radiation, vegetation, snow cover, ground thermal properties, surface relief and subsurface drainage. The factors for different conditions are determined empirically and some typical values are reported in [13]. For the calculations here, the thawing factor value of $n_t = 1$ is assumed to be reasonable.

The volumetric latent heat L can be expressed as

$$L = \rho_d L_f \frac{w - w_u}{100} \tag{2.4}$$

where ρ_d is the dry density of the soil, L_f is the specific latent heat of fusion (the amount of energy absorbed when a unit mass of ice is converted into a liquid at the melting point; typically, 333.7 kJ/kg), w is the total water content and w_u is the unfrozen water content of the frozen soil. For soils with little or no unfrozen water (such as sands and gravels), the unfrozen water content is usually very small. For many practical problems, assuming $w_u = 0$ will give acceptable L values for the active layer thickness calculation.

The active layer thickness is calculated for the locations of interest in Longyearbyen based on the temperature data presented earlier and the Stefan Solution described above. Based on experimental measurements at a selected location, the unfrozen thermal conductivity, the dry density and the total water content were estimated to be $\lambda_u = 1.8$ W/m/K, $\rho_d = 1800$ kg/m³ and $w = 30$ %, respectively; [15]. The progression of the active layer thickness with time is shown in Figure 5. The air thawing indices based on inferred daily temperatures are used for the calculation.
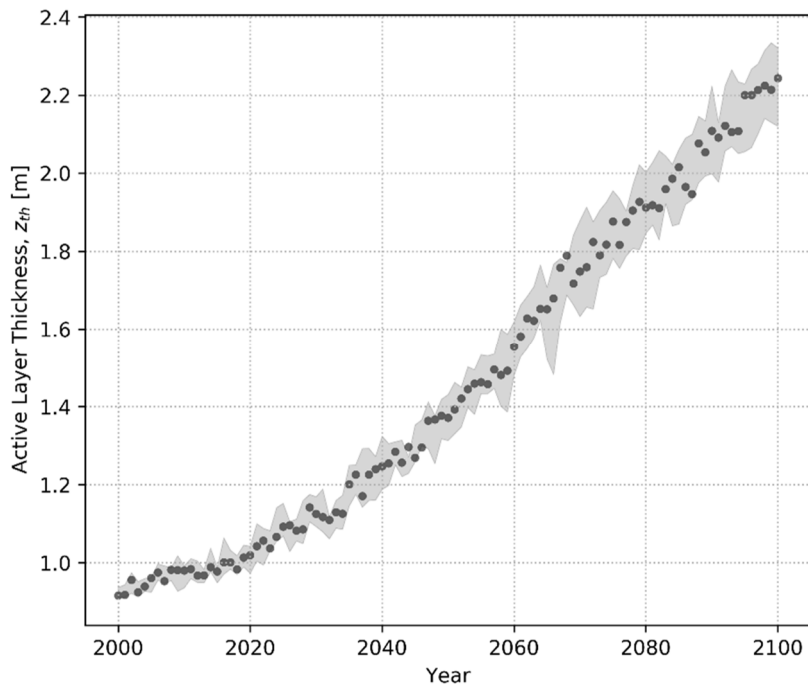
Figure 5: Progression of active layer thickness with time.

It can be seen from the plot that the thickness of the active layer increases, corresponding to the air temperatures forecasts, from around 1 m in the present day to more than 2 m after several decades. The rising temperatures not only increase the thickness of the active layer but also increase the temperature in the permafrost. The warming of the permafrost is discussed in the following section.

2.3   Ground Temperature: Numerical Simulations

The evolution of the ground temperature with time is studied based on numerical simulations. The GeoStudio package Temp/W is used to perform these simulations. The model step, model conditions and results are discussed in the following sections.

2.3.1 Model Geometry and Mesh

A typical idealized slope geometry is used here for the thermal analyses. The slope angles vary at the different locations of interest in Longyearbyen. For the simulation of the ground thermal regime using Temp/W, the slope angle does not have an effect on the outputs. The dimensions of the idealized slope are shown in Figure 6.

The model is spatially discretized with an average element size of 0.5 m. As the current problem set up does not involve complex initial/boundary conditions and material properties, numerical problems are not anticipated and a uniform mesh size is used throughout the model.
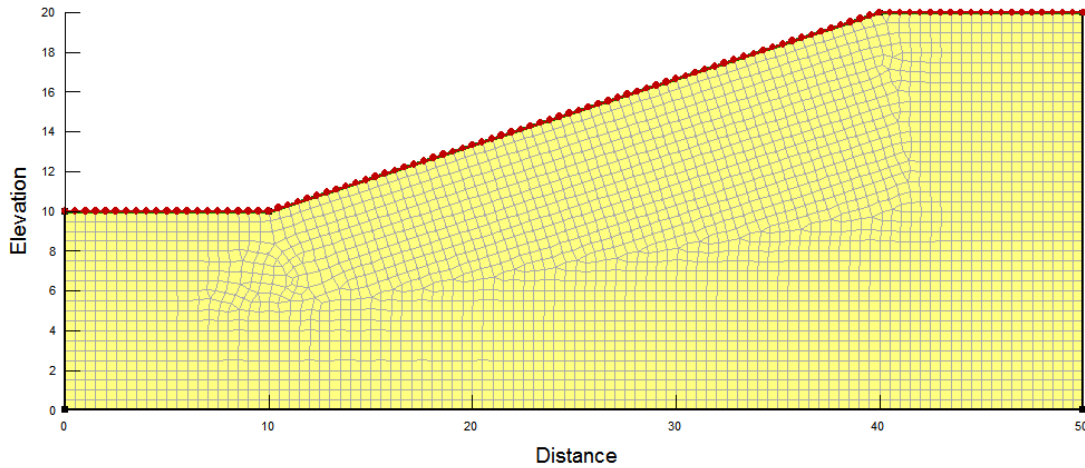
Figure 6: Model geometry and mesh used for the representative thermal analysis.

2.3.2 Material Properties

A full thermal model is used to model the material properties in Temp/W. The material properties used are given in Table 1.

Table 1: Material properties used for thermal analyses in Temp/W.

Parameter	Value	Unit
Unfrozen Thermal Conductivity	1.8	W/m/K
Frozen Thermal Conductivity	1.6	W/m/K
Unfrozen Specific Heat Capacity	3700	kJ/m^3/K
Frozen Specific Heat Capacity	1440	kJ/m^3/K
Dry Density of Soil	1800	kg/m^3
Total Water Content	30	%

For simplicity of the thermal analyses, a homogeneous soil body is assumed for the model here.

2.3.3 Initial and Boundary Conditions

The simulations are aimed at showing the evolution of the ground temperatures in the active layer and the permafrost based on the predicted temperature data. To demonstrate this, the thermal analyses are performed for the period from 2001 – 2050. The air temperature data for the year 2000 is used to generate the initial conditions for the subsequent analyses. The daily mean air temperature data for the year 2000 is shown in Figure 7. The mean annual temperature is used as the activation temperature for the initial analyses.

The existing air temperature data and forecast is applied as a thermal boundary condition at the ground surface. A step function is generated based on the seasonal mean temperatures for the targeted period of analysis. A plot of the step function for the period of analysis and a close-up for the first few years is shown in Figure 8. Natural thermal boundary conditions are assumed at the left, right and bottom boundaries of the model.
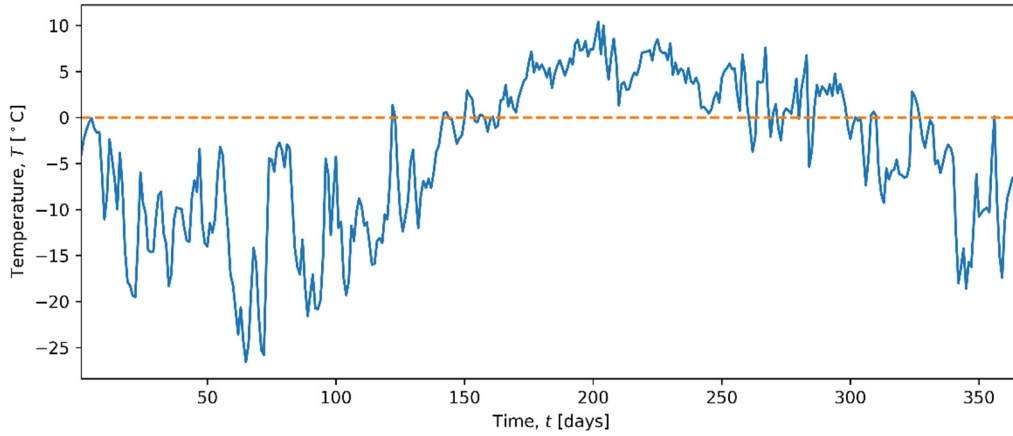
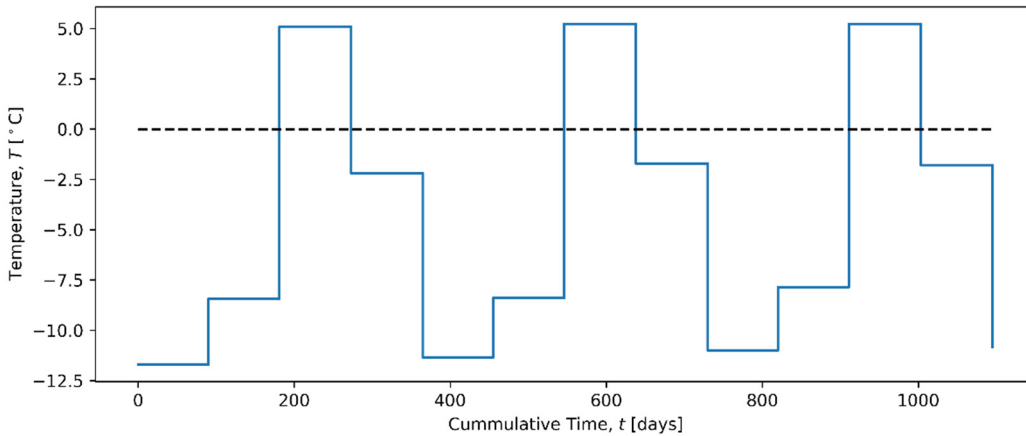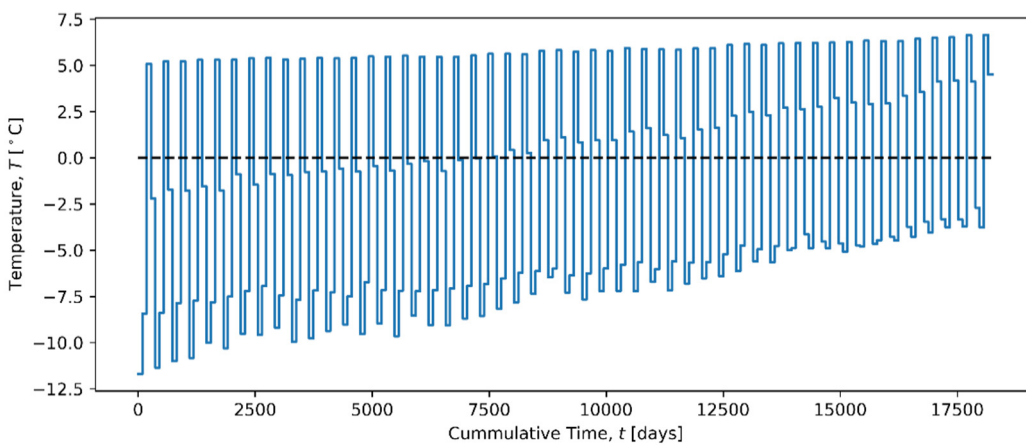Figure 7: Longyearbyen daily mean air temperature data for the year 2000.

Figure 8: Thermal boundary condition based on seasonal mean temperatures as a step function for the period of analysis (top) and a close-up for the first three years (bottom).

2.3.4 Results

The ground temperature profiles for selected years are shown in terms of contour plots in Figure 9 to Figure 12. The figures are shown at the end of the thawing season for each year, where the time points vary depending on the temperature data of the year in question. We observe from the results that, as predicted by analytical calculations, the active layer thickness increases with time based on the temperature forecast. The results also show that the

permafrost underneath the active layer gets warmer over the years. This gives an indication on the evolution of the ground thermal regime based on the simplified and homogenized analyses performed here. The trends of this evolution may be expected to be similar for various ground conditions in Longyearbyen. The temperature profiles versus depth for the selected years are shown in Figure 13.
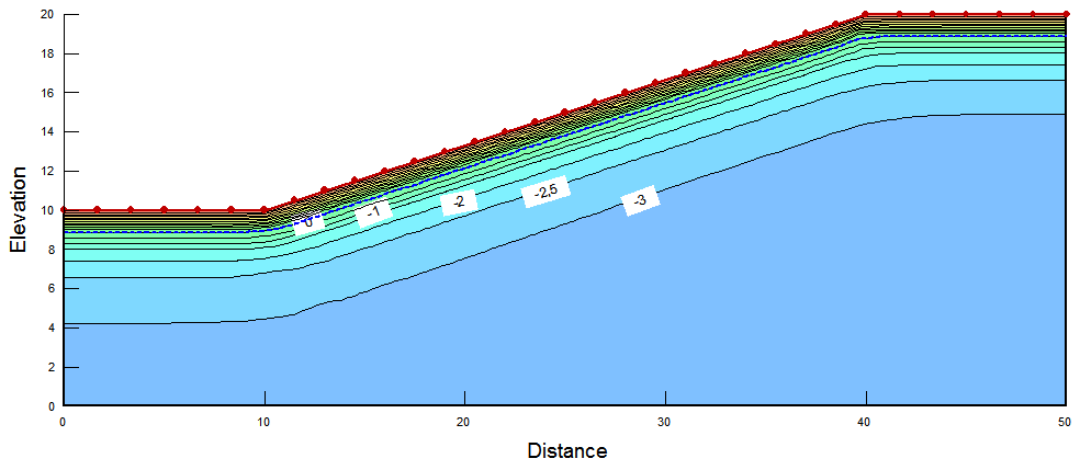

Figure 9: Ground temperatures at the end of the thawing season in the year 2020.

Figure 10: Ground temperatures at the end of the thawing season in the year 2030.

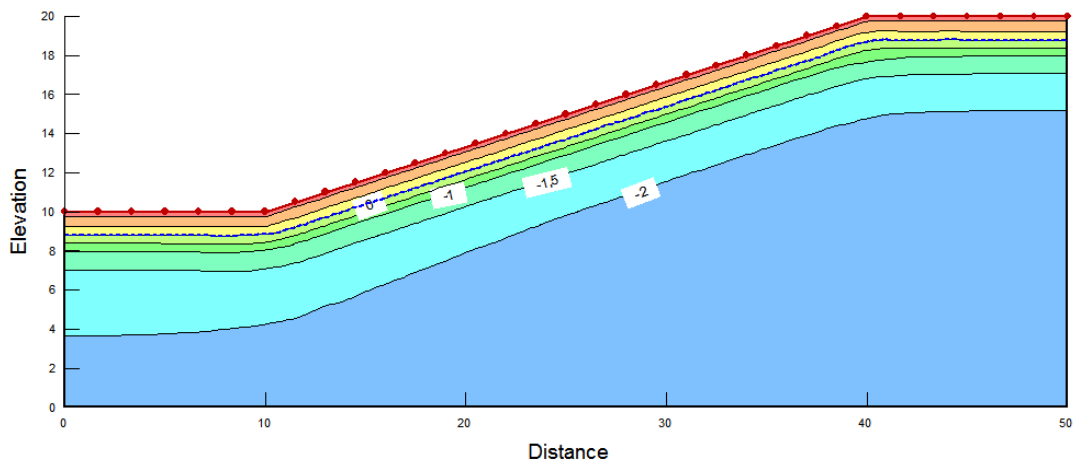Figure 11: Ground temperatures at the end of the thawing season in the year 2040.
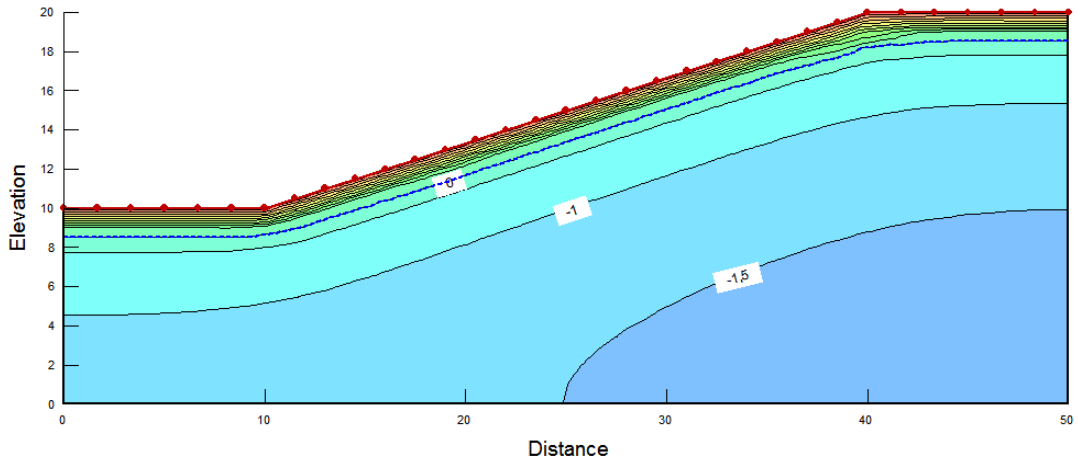
Figure 12: Ground temperatures at the end of the thawing season in the year 2050.

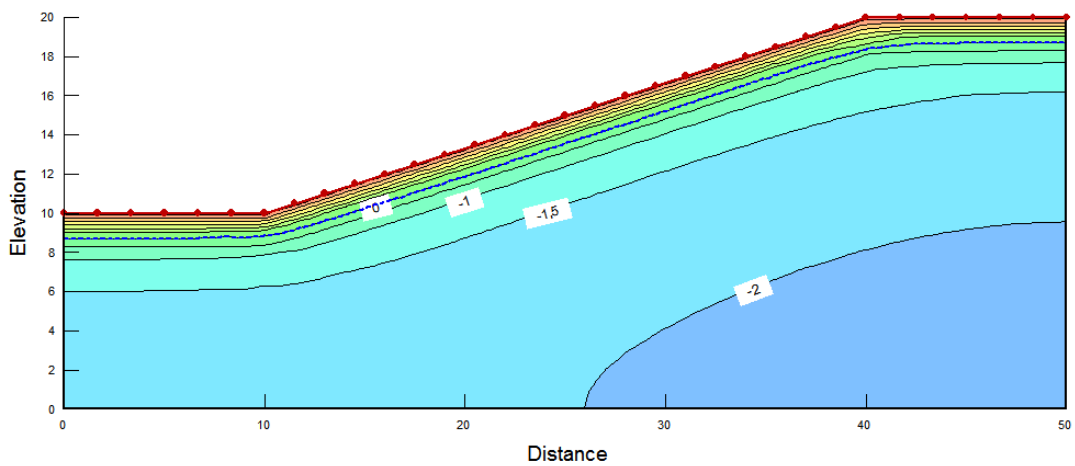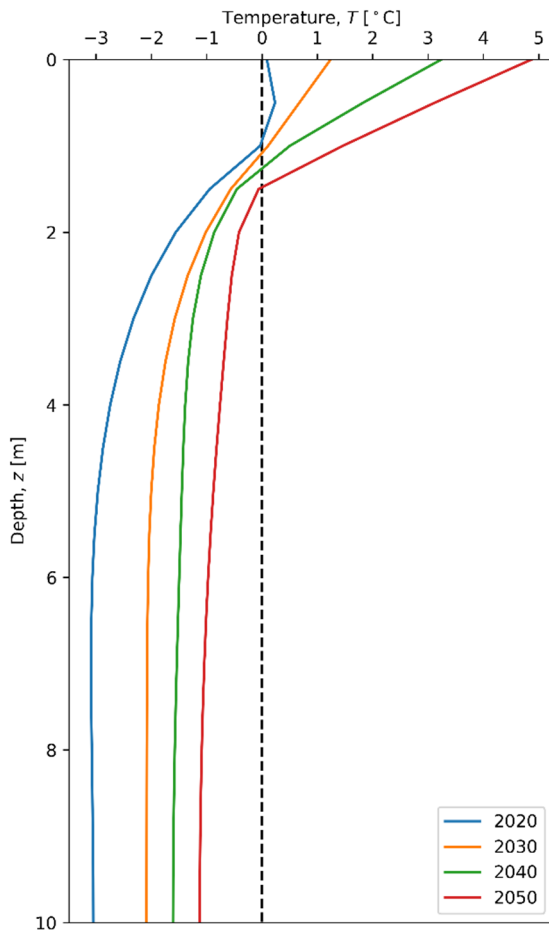Figure 13: Ground temperature profiles for selected years. The profiles are shown at time points when the thawing season ends and the next freezing period starts. These time points vary for the selected years depending on their respective temperature data.

2.4 Summary

The projected climate data show that temperatures will keep rising in Svalbard. Based on the analytical and numerical studies performed for the projected temperature data, it is observed that the active layer thickness will increase up to 2 m or more, depending on the thermal properties of the soil. The increase in ground temperatures also results in the warming of the permafrost underneath the active layer. The stability of slopes and the bearing capacity of existing infrastructure foundations is expected to be significantly affected by these changes.

3 Slope Stability Evaluation

The stability of a selected slope in Longyearbyen is studied. The effects of climate change and material properties are investigated and discussed in the following sections.

3.1 Location of Slope

The location of the slope selected for a case study is shown in Figure 14. The slope profile is extracted from [16] based on the cross-section line shown in the figure.
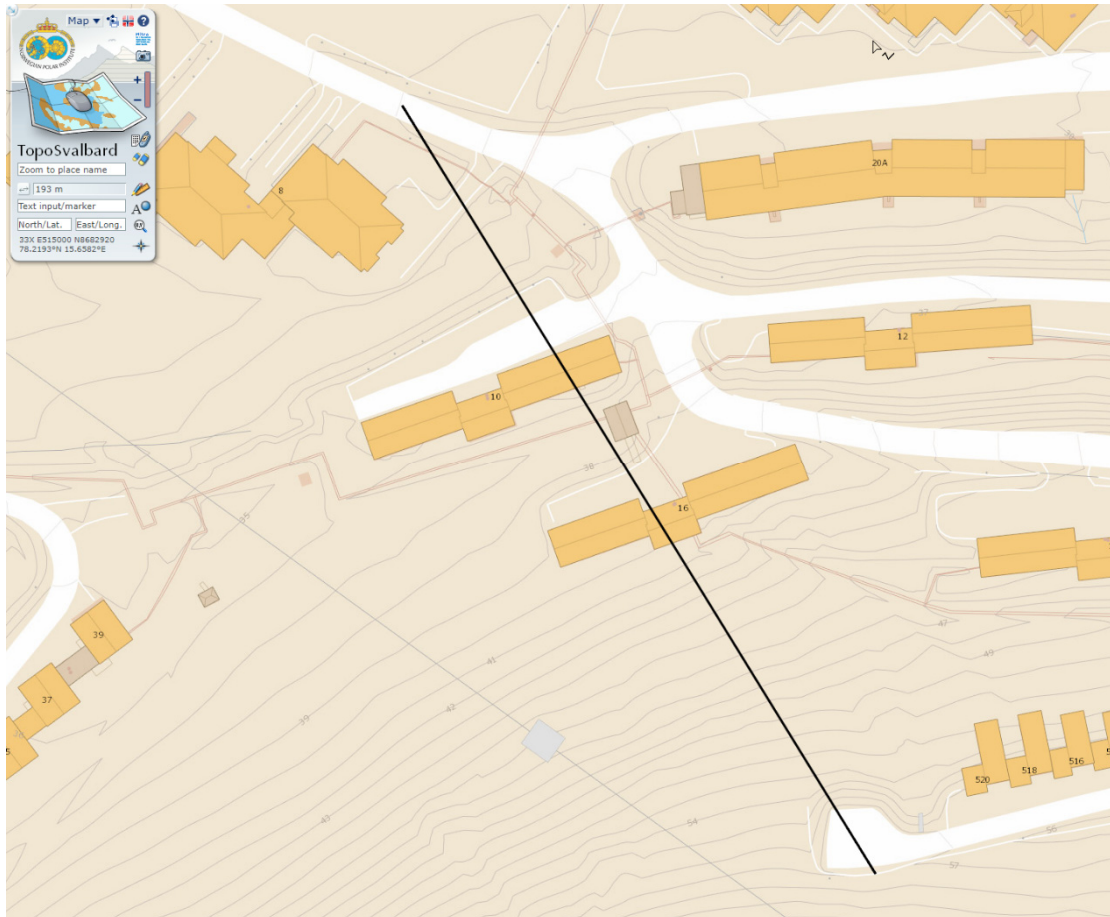
Figure 14: Location of slope and cross-section considered for a slope profile. Map: [34].

The stability of the slope is evaluated for changing climate by considering varying active layer thicknesses. Specifically, active layer thicknesses of 1.0 m, 1.5 m and 2.0 are considered and the models for these are shown in Figure 15, Figure 16 and Figure 17, respectively. The evaluations are performed using the software SLIDE which is based on limit equilibrium methods.

The material parameters used for the analyses are based on the index properties obtained from the project field and laboratory investigations. For drained analyses a cohesion of 3.5 kPa and a friction angle of 25° are assumed as reference values for the active layer. For the undrained case, a surface undrained shear strength of 5 kPa and a shear strength change with depth of 2 kPa/m are assumed as reference values. Conditions of excess pore pressure are simulated in a simplified and indirect manner by increasing the self-weight of water by 15%.

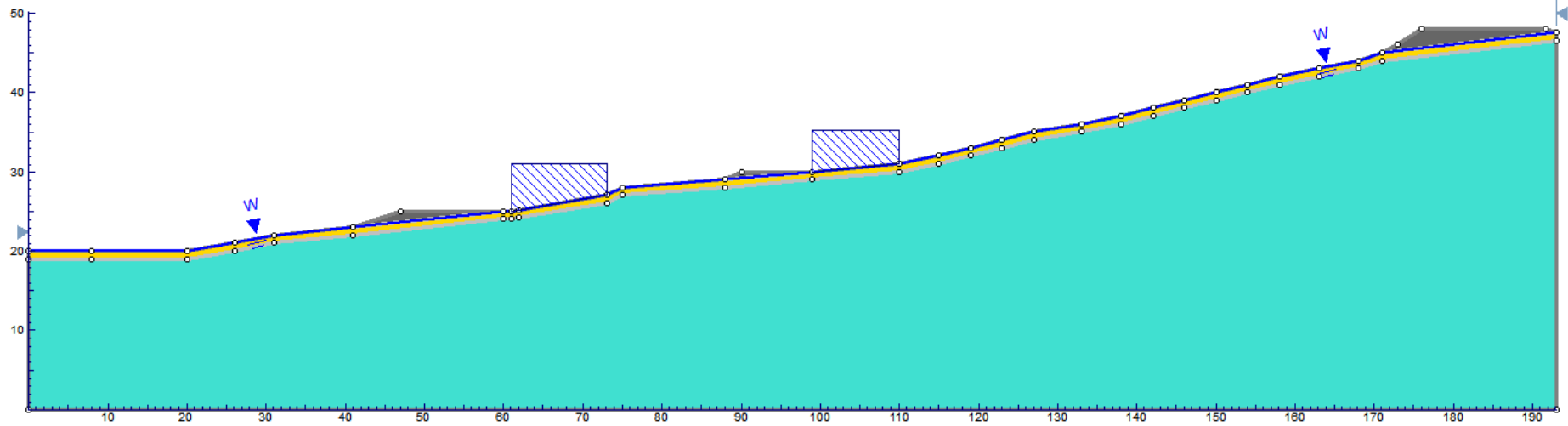Figure 15: Slope profile with a 1.0m thick active layer thickness, including gravel berms and illustration of buildings.
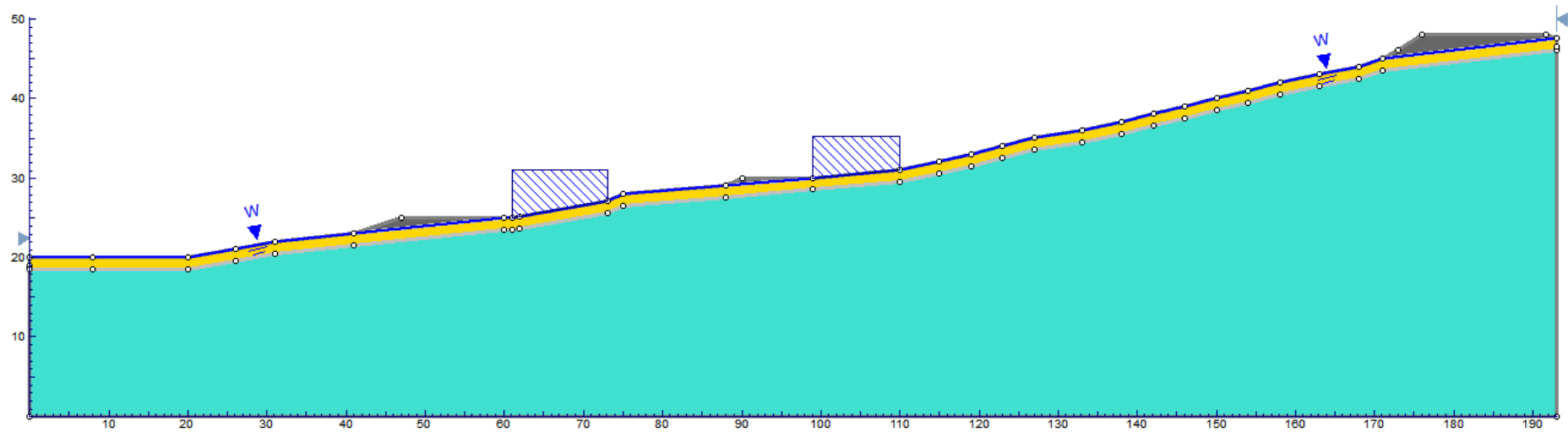
Figure 16: Slope profile with a 1.5m thick active layer thickness, including gravel berms and illustration of buildings.
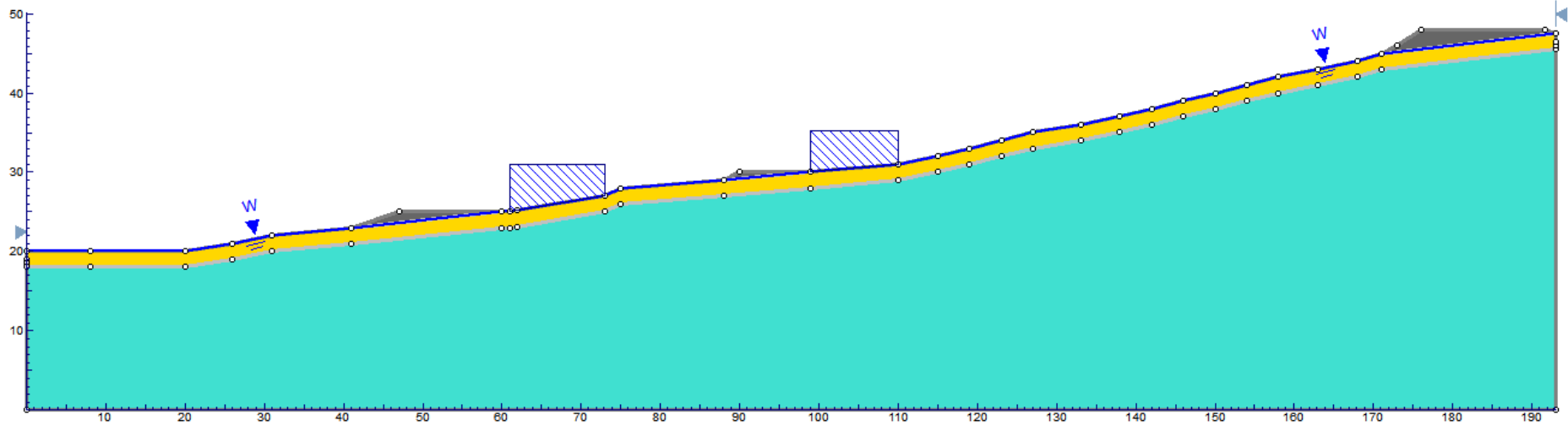
Figure 17: Slope profile with a 2.0m thick active layer thickness, including gravel berms and illustration of buildings.

3.2 Effect of Climate Change

The effect of climate change is considered in terms of an increasing active layer thickness. Active layer thicknesses of 1.0 m, 1.5 m and 2.0 m are considered. For simplicity, the active layer thicknesses are assumed to have a uniform thickness along the slope profile; these may be slightly different under insulating conditions such as gravel berms. The variation of the factor of safety with active layer thickness under drained and undrained conditions is shown in Figure 18. A similar variation under sudden shear strength reduction is shown in Figure 19.
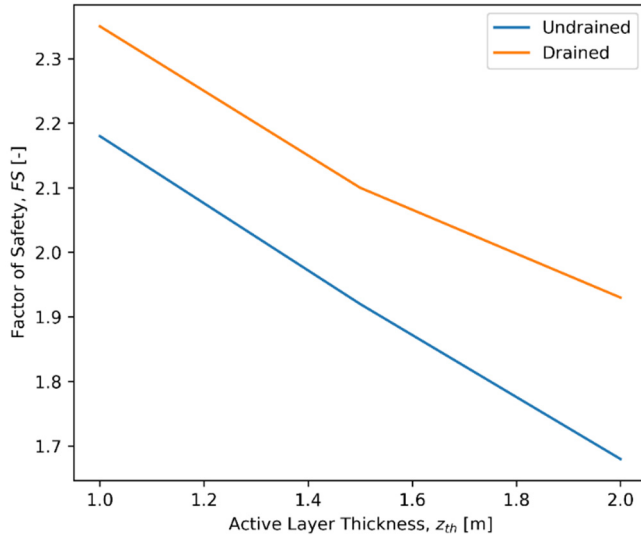
Figure 18: Factor of safety versus active layer thickness under drained and undrained conditions.
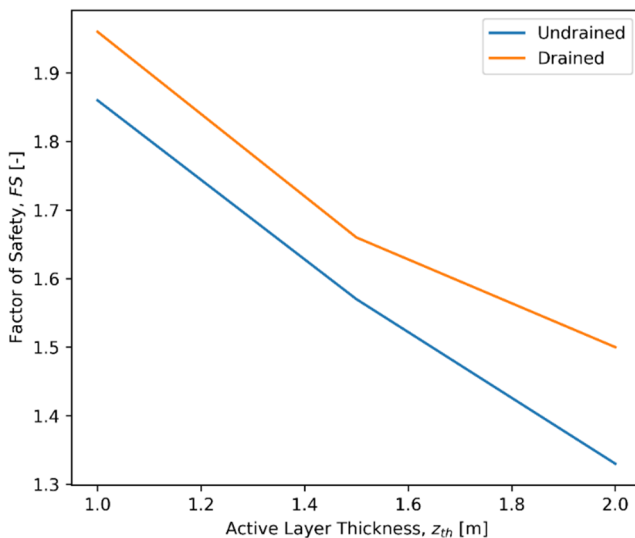
Figure 19: Factor of safety versus active layer thickness under sudden shear strength reduction due to precipitation or other instantaneous loading.

3.3 Sensitivity to Material Parameters

The effect of the key material parameters on the factor of safety is investigated through sensitivity analyses. The sensitivity of the factor of safety to the cohesion and friction angle, relevant for drained analyses, is shown in Figure 20. A similar plot illustrating the effects of undrained shear strength and its increment with depth is shown in Figure 21. The sensitivity analyses are performed with a 2 m active layer thickness as a reference.
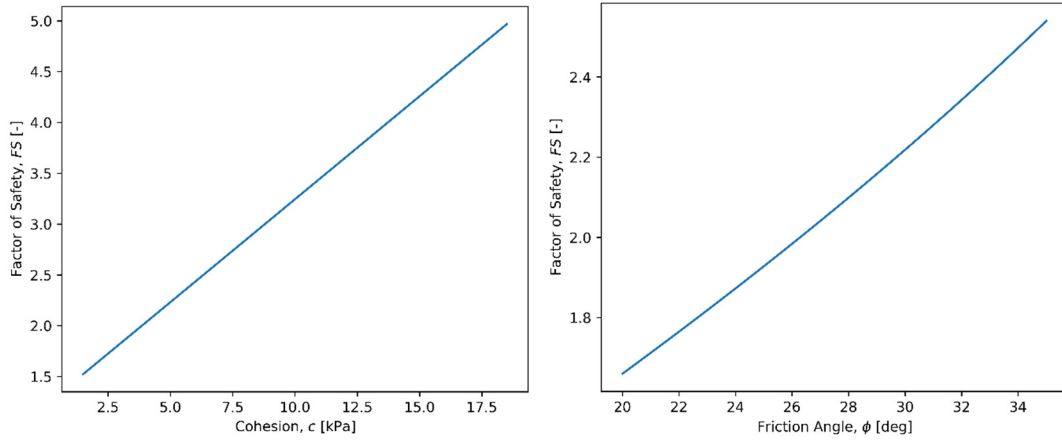
Figure 20: Effects of the cohesion and friction angle of the active layer on factor of safety. The reference value of the friction is applied when varying the cohesion and vice versa.
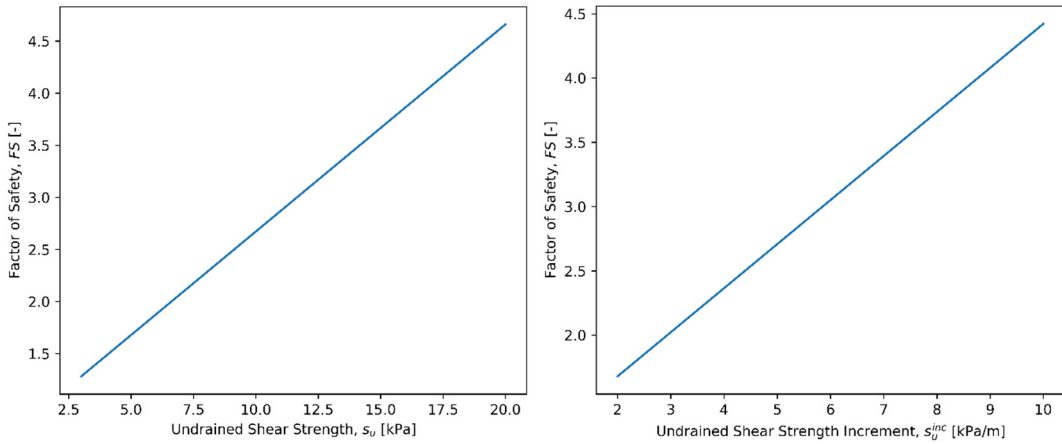
Figure 21: Effects of the surface undrained shear strength of the active layer and its increment with depth on factor of safety. The reference value of the undrained shear strength is applied when varying its increment and vice versa.

Note that the safety factors reported so far are intended to give an indication of the effect of climate change and the variation of material parameters. Various assumptions are made in the calculations and the numbers should not be taken as explicitly conclusive. The observed trends are, however, expected to hold under different circumstances.

3.4   Summary

Slope stability evaluations were performed for a representative slope in the study area by considering changing active layer thicknesses according to the projected ground temperature regime. The factor of safety against slope failure decreases with increasing active layer thickness. Under the specific assumptions made for the evaluation, the representative slope was found to be stable for active layer thicknesses of up to 2m. Sensitivity analyses show that the factor of safety is significantly affected by changes is material parameters such as cohesion and friction angle, which are associated with the ground thermal regime. Accurate estimation of material properties is required for a definitive slope stability evaluation.

4   Laterally Loaded Piles on a Slope

Pile foundations may be subjected to lateral loading in various ways. One such way is the downward movement of soil on a slope for piles installed on a sloping ground. In cold regions, the downward movement of soil may be caused by a process known as solifluction, which is briefly discussed below. In subsequent sections, the capacity of piles subjected to such lateral loading is investigated through analytical calculations and numerical simulations.

4.1   Solifluction

Solifluction is defined as a slow downslope flow of saturated unfrozen earth materials according to the glossary of permafrost by [26] where one component could be creep of frozen ground. When the soil above the permafrost is thawed, which is the active layer, the water in the soil becomes trapped because the underlying permafrost is considered to be impermeable. This leads to oversaturation in the active layer and a downward slide occurs under the pull of gravity. The rate of solifluction may vary depending on several factors. Climate change affects the ground thermal regime through frequent freeze-thaw cycles and increased active layer thicknesses, thereby increasing the rate of solifluction. Some studies, such as [27], claim that solifluction movements are a result of frost heaving and subsequent thawing and that creep is not a significant part of the process.

Infrastructure built on slopes susceptible to solifluction will be subjected to forces due to the downward movement of the soil in the active layer. Thus, the additional forces that results from solifluction should be accounted for in the design of these infrastructure.

For structures designed and built without considering the effect of solifluction, the serviceability during the lifetime of the structures must be investigated to take the necessary counter measures in the face of climate change.
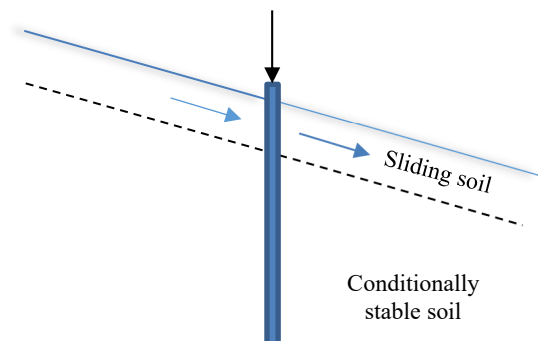
Figure 22: Illustration of soil downward movement on a slope due to solifluction.

Pictures illustrating soil movement around a pile foundation due to solifluction can be referred from [27], where loss of pile-soil contact on the passive side of the pile is demonstrated.

A specific focus of the current study is buildings in Longyearbyen supported by pile foundations on sloping terrains. An illustration of the downward movement of soil on a slope where piles are installed is shown in Figure 22. We aim to investigate the effect of solifluction on the lateral capacity of piles. The study is performed in a generic way such that the results can serve to assess the serviceability of existing buildings and add knowledge for the design of future buildings. The theory of laterally loaded piles is first discussed and analytical and numerical calculations are then performed for piles on a slope subjected to lateral loads due to soil movement.

4.2 Theory of Laterally Loaded Piles

When a pile is subjected to lateral loading, the earth pressure distribution around the pile changes as illustrated in
Figure 23. As the pile deflects, the stresses on the backside of the pile decrease whereas the stresses increase on the front, if there is no loss of contact between the pile and the soil.
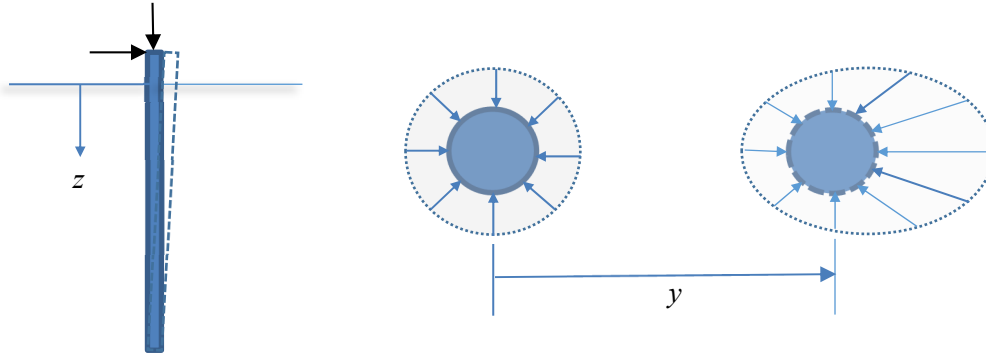
Figure 23: A pile subjected to lateral loading and soil stress distribution around the pile before and after deflection.

Laterally loaded piles in soil are usually analysed by developing a nonlinear relationship between the soil resistance (p) and the pile head deflection (y), resulting in the so-called p-y curve. A beam model is usually used to develop this relationship. The general differential equation of this model is given by

$$E_p I_p \frac{d^4 y}{dz^4} + P_z \frac{d^2 y}{dz^2} + E_{py} y - Q = 0 \tag{4.1}$$

where $E_p I_p$ is the bending stiffness of the pile, y is the lateral deflection, z is the depth along the pile, P_z is the axial load on the pile, E_{py} is the soil reaction modulus and Q is any distributed load along the length of the pile. The soil reaction modulus is obtained from a p-y curve as illustrated in Figure 24 . For piles subjected to lateral loading due to a sliding soil, as in the case of solifluction, the beam model equation is modified to account for the movement of the soil. The modified equation is

$$E_p I_p \frac{d^4 y}{dz^4} + P_z \frac{d^2 y}{dz^2} + E_{py} (y - y_{soil}) - Q = 0 \tag{4.2}$$

where $y - y_{soil}$ represents the relative pile-soil movement and E_{py} in this case is obtained from the p-y curve adjusted for soil movement.

Figure 24: p-y curves in a stable (left) and sliding soil (right).
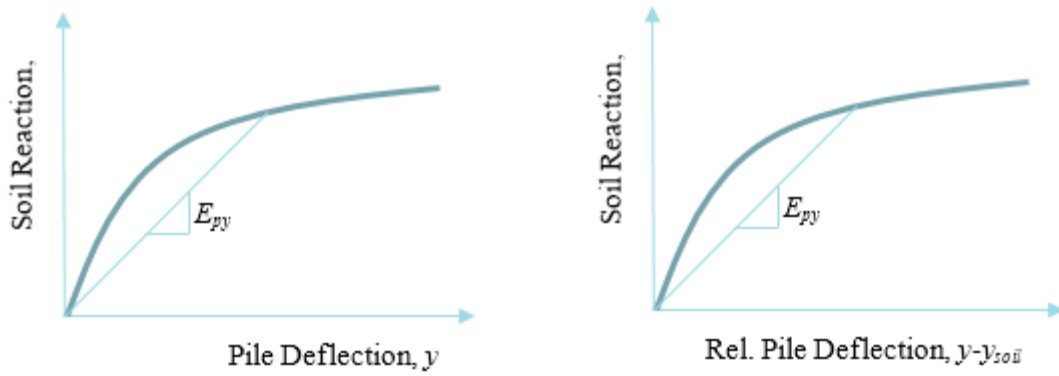
4.3   p-y Curves for Frozen Soil

The development of p-y curves is, in general, dependent on the soil type and loading conditions. It is usually assumed that the stress-strain curve for soil from experiments and the p-y curve of soil response have similar shapes. The first step in constructing p-y curves is to calculate the ultimate soil response per unit depth of pile length. This for frozen soil, according to [28], may be calculated from

$$p_{ult} = N_p c D \qquad (4.3)$$

where N_p is the ultimate bearing capacity coefficient, c is the soil shear strength and D is the pile diameter or width. The bearing capacity coefficient increases with depth and may be calculated from

$$N_p = 3 + \frac{\sigma_v}{c} + \frac{Jz}{D} \qquad (4.4)$$

where σ_v is the vertical overburden pressure at depth z, J is an empirical coefficient with a typical value of 0.5 and z is the depth below ground level. The p-y curve is then approximated by the parabola

$$p = \frac{1}{2} p_{ult} \left(\frac{y}{y_{50}}\right)^{\frac{1}{n}} \qquad (4.5)$$

where p is the soil reaction to a lateral pile deflection, y is the lateral pile deflection and y_{50} is the lateral deflection at which $p = p_{ult}/2$ and n is a stress-strain exponent. The value of y_{50} can be approximately calculated from

$$y_{50} = 2.5\varepsilon_{50}D \qquad (4.6)$$

where ε_{50} is the strain at one-half of the ultimate soil strength. A typical value of $\varepsilon_{50} = 0.25\%$ is used for the short-term strength and increased for the long-term depending on various factors. Suggested values of ε_{50} for fine- and coarse-grained soils may be referred from [28].

4.4   Analytical Calculations

The capacity of piles subjected to lateral loading is investigated here based on analytical approaches discussed previously. For the pile foundations of interest in this study, besides the type of lateral loading and soil type, one of the main factors that affects the pile capacities is climate change. This affects pile foundations in various ways. Increasing active layer thicknesses associated with solifluction are expected to add to the lateral loading of piles. In

addition, the continued warming of the permafrost is anticipated to affect the magnitude of the soil reaction. Slope angle is the other factor that affects the capacity of pile on installed on a sloping ground. These two factors are investigated quantitatively in the following sections.

4.4.1 Effect of Climate Change

The strength of frozen soil, as known, is strongly dependent on temperature and other temperature dependent volumetric properties. Increased ground temperatures and recurrent freeze-thaw cycles due to climate change increase the thickness of the active layer (as shown in earlier sections) and reduce the long-term strength of the frozen soil. This in turn results in the reduction of the ultimate capacity of piles in frozen soils.

In a Mohr-Coulomb type interpretation of soil shear strength, the soil cohesion and effective angle of internal friction are the key parameters. The shear strength of frozen soil τ_f can thus be written as

$$\tau_f = c_f + \sigma_v' \tan \phi_f \tag{4.7}$$

where c_f is the cohesion of frozen soil, σ_v' is the effective overburden stress and ϕ_f is the effective angle of internal friction of frozen soil. For frozen soils at very low temperatures, the effective friction angle is usually negligible as increasing volumetric ice content binds the soil particles together. On the other hand, the soil cohesion increases significantly with decreasing temperature and increasing volumetric ice content. Thus, the shear strength of frozen soils is mainly governed by the cohesive strength, especially for fine-grained soils.

The frozen cohesive strength may be expressed as a function of temperature and volumetric ice content. One such expression proposed by [29] is given by

$$c_f = c_t + \frac{\rho_w L_f}{T_f} \langle T_f - T \rangle^{1-\alpha} \left(\frac{n_o - w_u}{n_o} \right)^{\beta} \tag{4.8}$$

where c_t is the thawed cohesion, ρ_w is the density of water, L_f is the latent heat of fusion, T_f is the reference freezing temperature, T is the actual temperature, n_o is the initial porosity, w_u is the unfrozen water content and α and β are model parameters. For frozen soils where the unfrozen water content is negligible, the equation reduces to

$$c_f = c_t + \frac{\rho_w L_f}{T_f} \langle T_f - T \rangle^{1-\alpha} \tag{4.9}$$

An illustration of the cohesive strength of frozen soil versus temperature is shown in Figure 25. The plots are made by assuming $c_t = 20$ kPa, $\rho_w = 1000$ kg/m³, $L_f = 334$ kJ/kg, $T_f = 273.15$ K, $n_o = 0.4$, $w_u = 0.05$ and $\beta = 3.0$. The cohesion increases significantly with decreasing temperature. The plot illustrates that warming of permafrost is associated with a drop in cohesive strength.
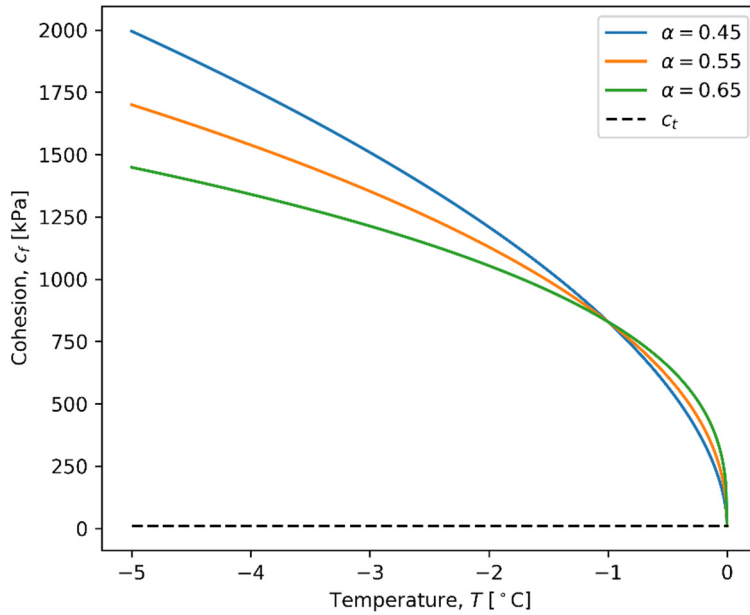
Figure 25: Cohesive strength of frozen soil as a function of temperature.

As discussed previously, the ultimate soil reaction in cohesive soils is proportional to the shear strength of the soil. This results in a significant difference in the *p-y* curves for the active layer and the permafrost underneath. A typical *p-y* curve at a certain depth in the active layer is shown in Figure 26. A pile diameter of 0.14 m is assumed for this and subsequent results, unless otherwise specified. The pile under lateral loading deflects the most within the active layer and this is reflected in the magnitude of the soil reaction given for the assumed cohesion and overburden stress. An increased active layer thickness implies an increased region of weak layer which may result in larger pile deflections for the same lateral loading.
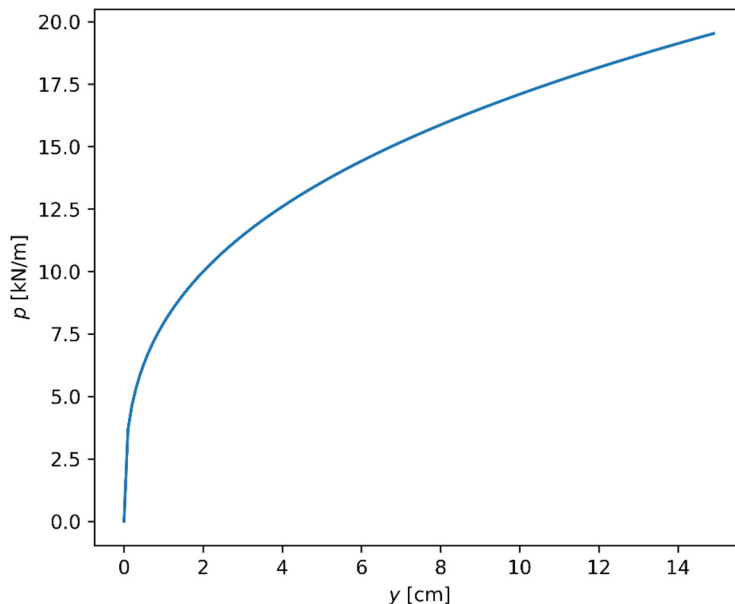

Figure 26: A typical p-y curve in the active layer (thawed soil).

Figure 27 shows *p-y* curves for permafrost at different temperatures. The plots are made at a similar depth, for the same overburden stress, and assuming the same pile geometry. The lateral force required to cause the same level of deflection decreases with increasing temperature.
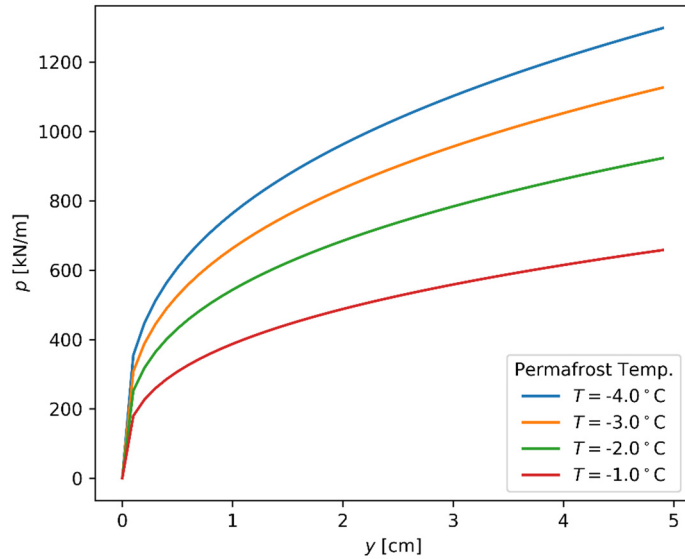
Figure 27: Permafrost p-y curves at different temperatures under similar conditions of overburden stresses and pile cross-sectional geometries.

4.4.2 Effect of Slope Angle

For piles installed on sloping terrains, the slope angle affects the ultimate lateral capacity and thus the resulting *p-y* curves. The effect of the slope angle on the ultimate pile capacity, according to [30], may be taken into account through

$$p_{ult} = N_p cD \left(\frac{1}{1 + \tan\theta}\right) \tag{4.10}$$

where θ is the slope angle. In the expression above, it is assumed that the soil in the active layer is fine-grained and the effect of cohesion is more significant compared to the effect of friction angle, which is negligible for frozen soils at very low temperatures.

The effect of slope angle on *p-y* curves is illustrated in Figure 28 for soil properties in the active layer. A significant reduction is observed in the ultimate pile capacity as the slope angle increases.
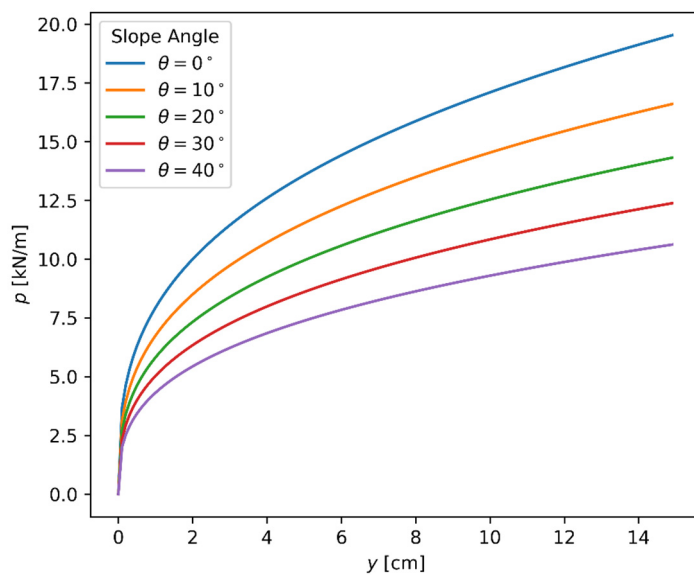

Figure 28: Effect of slope angle on the lateral capacity of piles. The plots are made for thawed soil properties corresponding to a typical active layer.

The ultimate pile capacity in permafrost also reduces with increasing slope angle, as shown in Figure 29. The shear strength of permafrost at different temperatures is considered with other factors being in a similar condition.
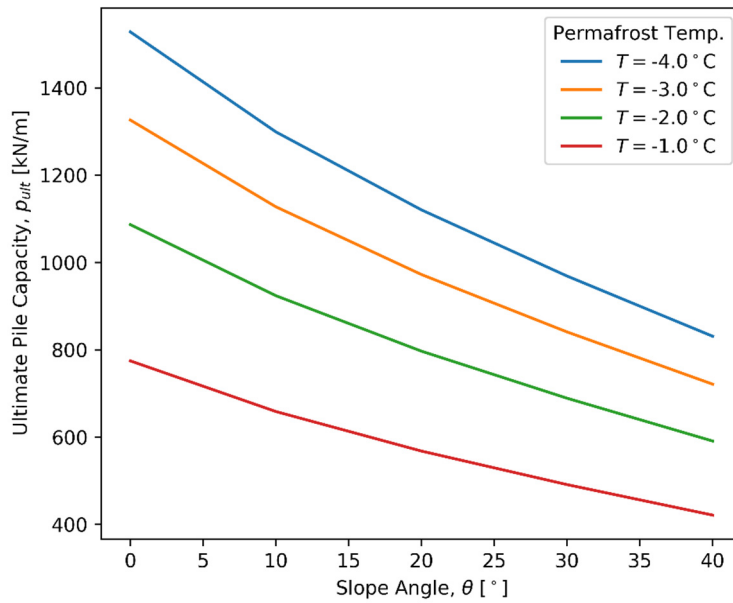
Figure 29: Effect of slope angle on the ultimate lateral capacity of piles in permafrost at different temperatures. The comparisons are made under similar conditions of overburden stress and pile cross-sectional geometries.

4.4.3 Effect of Pile Diameter

For fine-grained soils, the ultimate soil reaction under lateral loading, as expected, is proportional to the pile diameter or width. The effect of pile diameter on soil response in the active layer is illustrated through the *p-y* curves in Figure 30.

Figure 30: Effect of pile diameter on the lateral capacity of piles.

4.5   Finite Element Simulations

It was shown through analytical calculations in the previous section that factors such as climate change, slope angle and pile geometry affect the lateral capacity of piles in frozen slopes. Finite element simulations are performed here to further study some aspects of these factors. In particular, the effect of cli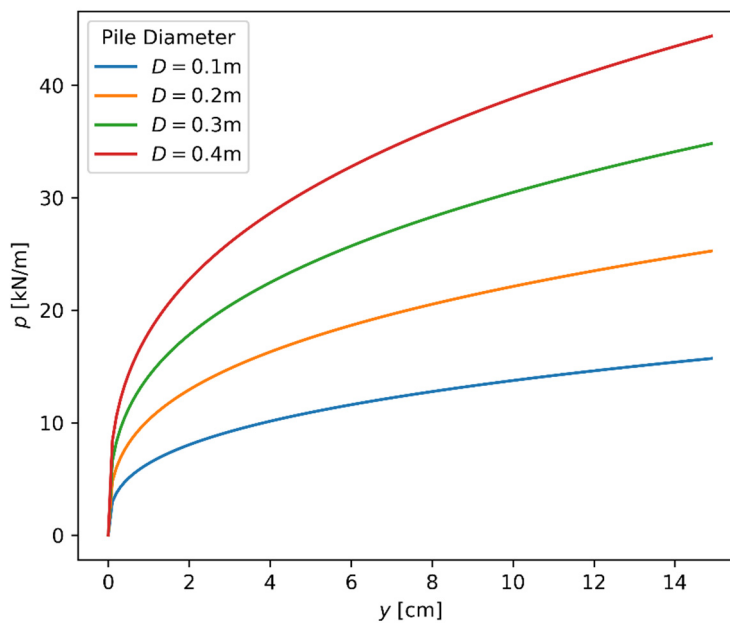mate change is considered through varying the active layer thickness with piles on slopes. The downward movement of soil due to solifluction is taken into account and the effect of this on the capacity of piles installed at different locations on a slope is investigated. The finite element software PLAXIS 2D is used for the simulations. The combined effect of these factors is analysed by quantifying pile head deflections and structural forces.

Model Geometry and Mesh

A numerical model with an arbitrary slope is setup with single piles at the middle and the toe of the slope. The model dimensions and the finite element meshes used for the analyses are shown in Figure 31, Figure 32 and Figure 33 for active layer thicknesses of 1.0m, 1.5m and 2.0m, respectively.
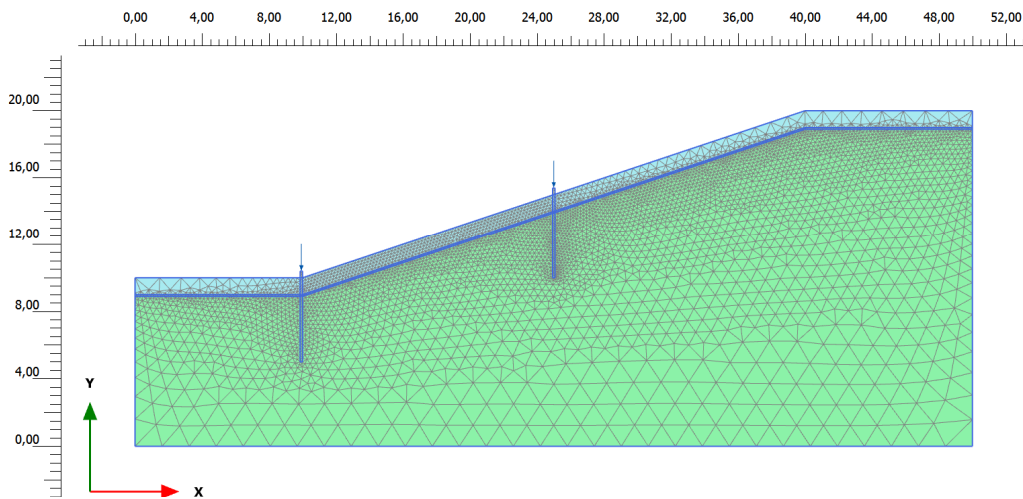

Figure 31: Finite element model dimensions and mesh with a 1.0 m thick active layer.
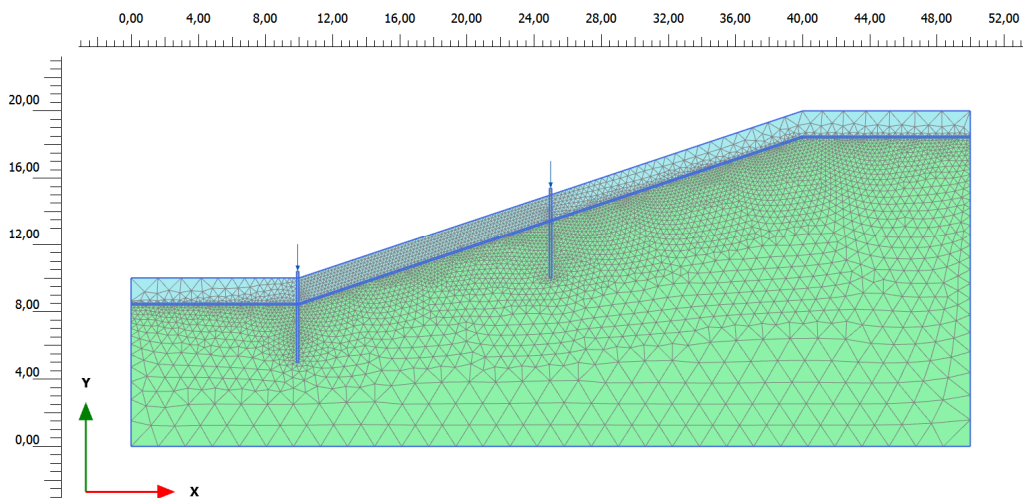

Figure 32: Finite element model dimensions and mesh with a 1.5 m thick active layer.
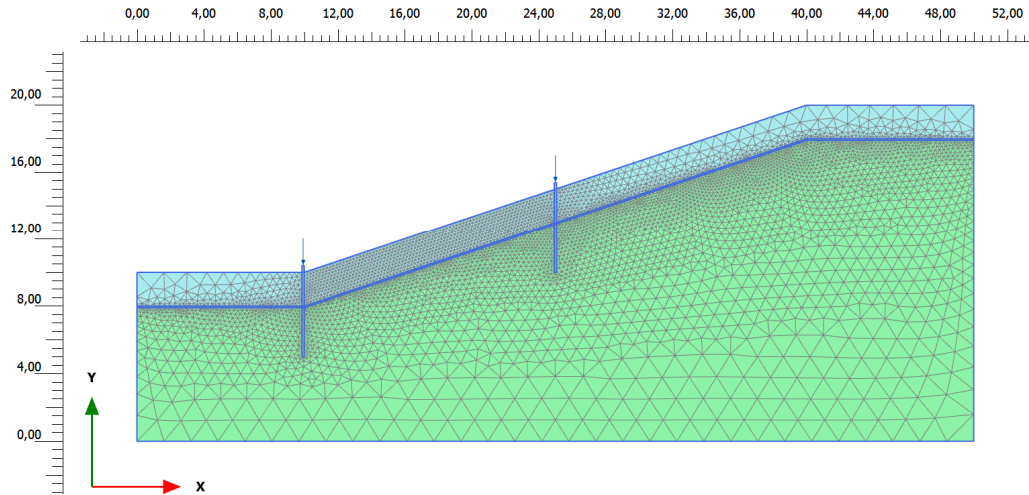
Figure 33: Finite element model dimensions and mesh with a 2.0 m thick active layer.

Axial loads are applied at the top of the piles to simulate the loads transferred from the superstructure to the foundation. For a typical residential house, the axial load transferred to a single pile is estimated to be in the range 50 – 100 kN, depending on the number of piles used for support. An axial load of 50 kN is assumed to act on a single pile for the simulations here.

Material Properties

The active layer and the permafrost underneath it are modelled using the Mohr-Coulomb model. For simplicity, the main material parameters are averaged for the layers. The temperature of the permafrost is considered in the estimation of its shear strength properties. We have seen earlier that the permafrost gets warmer as the active layer thickness increases, thus reducing its shear strength.

The piles are modelled using a linearly elastic material. Square hollow steel piles are commonly used nowadays for construction of buildings in Longyearbyen, [15]. A width of 140 mm and a wall thickness of 8 mm are used for the pile dimensions. The piles are assumed to be embedded up to 5 m in the permafrost. The Young's modulus and Poisson's ratio of steel are set to 200 GPa and 0.3, respectively. The stiffness of the pile is reduced in the input considering that the simulations are performed in 2D plane strain; see [31].

Model Conditions

We aim to investigate the lateral loading on piles due to the downward movement of the active layer i.e. solifluction. Solifluction is a time dependent process and the rate of downward movement at a certain location varies depending on several factors. It is anticipated that the maximum rates of solifluction occur during the thawing season when the active layer thickness is at its maximum resulting in the highest build-up of excess pore pressure in the soil. The excess pore pressure is dissipated gradually and this decreases the rate of solifluction afterwards. For the active layer thicknesses of 1.0 m, 1.5 m and 2.0 m considered here, downward movement of the soil on the slope is initiated by introducing a thin weak shear zone between the active layer and the permafrost.

Two pile locations, one at middle of the slope and one at the toe, are considered. A pile at the crest is not considered here; the maximum lateral force exerted on a pile at the crest will be in the same order or lesser than on a pile at mid slope depending on where downward movement is initiated; see [32].

Results

The results from the analyses are presented in the following in terms of pile head deflections and bending moments in the pile. These are discussed based on climate change and pile location on slope as the main factors.

4.5.1 Effect of Climate Change

In the event of the downward movement of soil on a sloping terrain, higher active layer thicknesses are clearly associated with a larger sliding soil mass. Thus, the lateral force exerted on the pile foundations increases with increasing active layer thicknesses, resulting in larger pile deflections and pile internal forces. These are quantified for the toe and mid piles in Figure 34 and Figure 35, respectively, for the three active layer thicknesses considered.

If the 1.0 m thick active layer is taken as a reference, a 50% increase in the active layer thickness results in approximately tripled pile head deflections, both for the toe and mid piles. On the other hand, a 100% increase in the active layer thickness results in more than a fivefold increase in the deflections of the toe and mid piles. The bending moments in the piles also increase corresponding to the increase in deflections. These findings are based on square hollow steel piles of the assumed dimensions used for the simulations. Similar rates of increase may be expected for piles made from other materials or having different cross-sectional geometries.

Figure 34: Steel piles - head deflections and bending moments of the toe pile under different active layer thicknesses.

4.5.2 Effect of Pile Location

The location of the pile determines the magnitude of lateral force sustained by the pile during the downward movement of soil. The lateral forces on piles installed at the middle of the slope are larger than on piles installed at the toe of the slope. These are again shown in terms of deflections and bending moments in Figure 34 and Figure 35 for the toe and mid piles,

respectively. Under the same conditions of material properties and pile geometries, the calculations here show that the pile at mid slope experience nearly doubled deflections and internal forces compared to the pile at the toe of the slope. Similar observations are expected to hold for different materials and pile properties. As discussed earlier, piles installed close to the crest of the slope are expected to experience varying lateral forces, up to the same order of magnitude as piles at mid slope, depending on where the downward movement of the soil is initiated.

4.5.3 Effect of Pile Material

A similar set of analyses are performed for piles made of timber. A circular cross-section with a diameter of 250 mm is assumed for the piles. The Young's modulus and Poisson's ratio of timber are set to 10 GPa and 0.3, respectively.

The head deflections and bending moments for the timber pile considered are shown in Figure 36 and Figure 37, for the toe and mid piles, respectively. We observe that the head deflections are significantly larger for timber piles when compared to steel piles, which is expected due to the lower Young's modulus of timber.

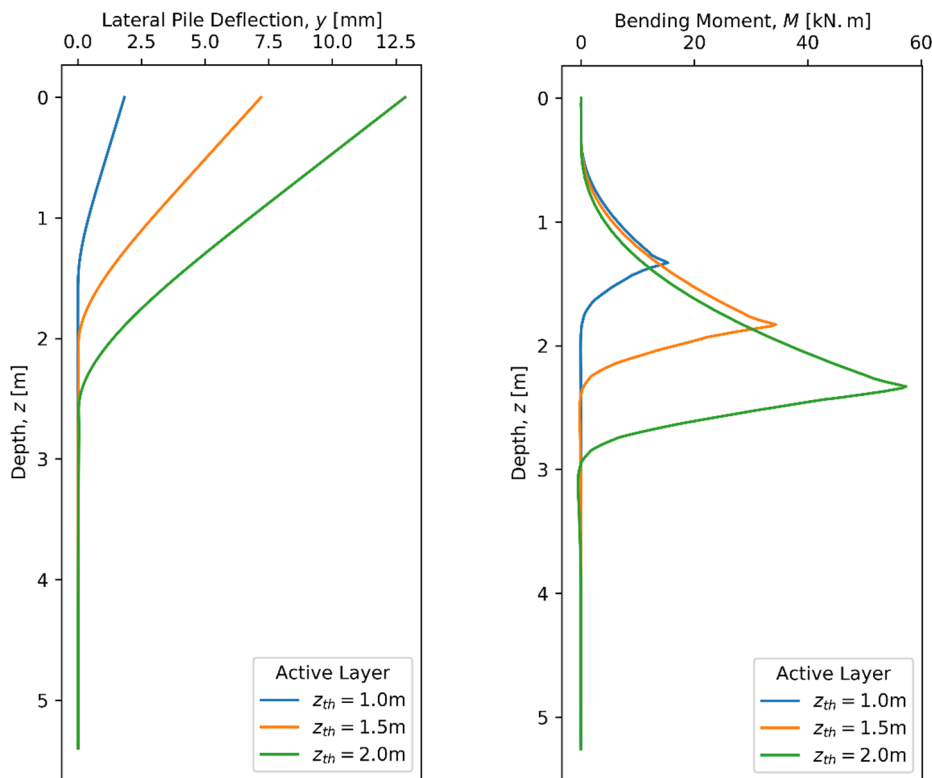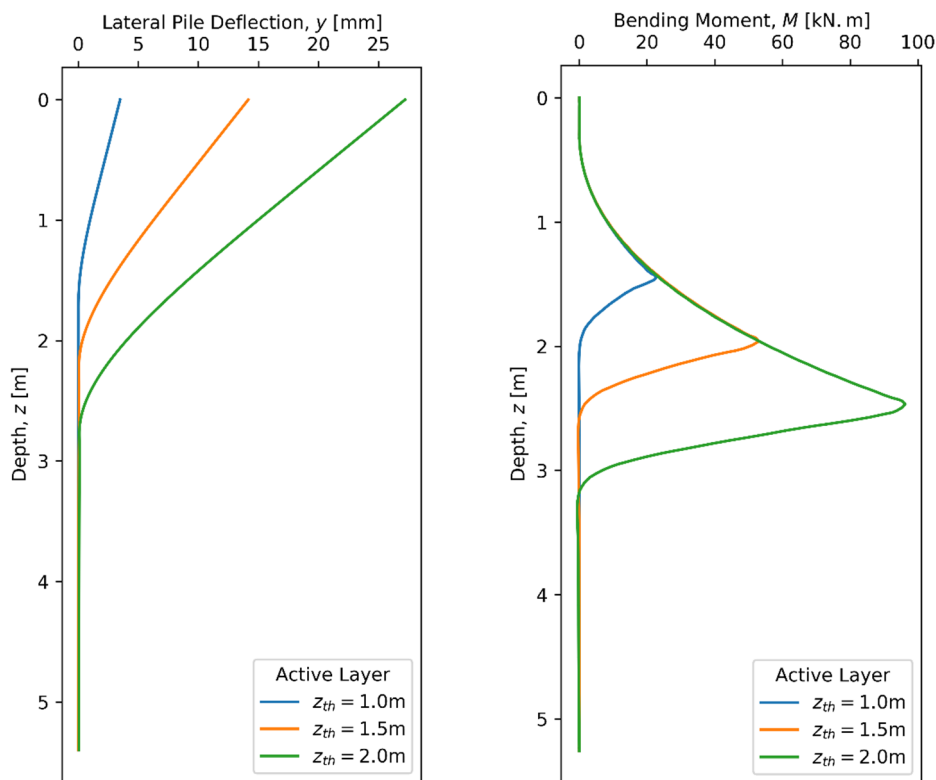Figure 35: Steel piles - head deflections and bending moments of the mid pile under different active layer thicknesses.
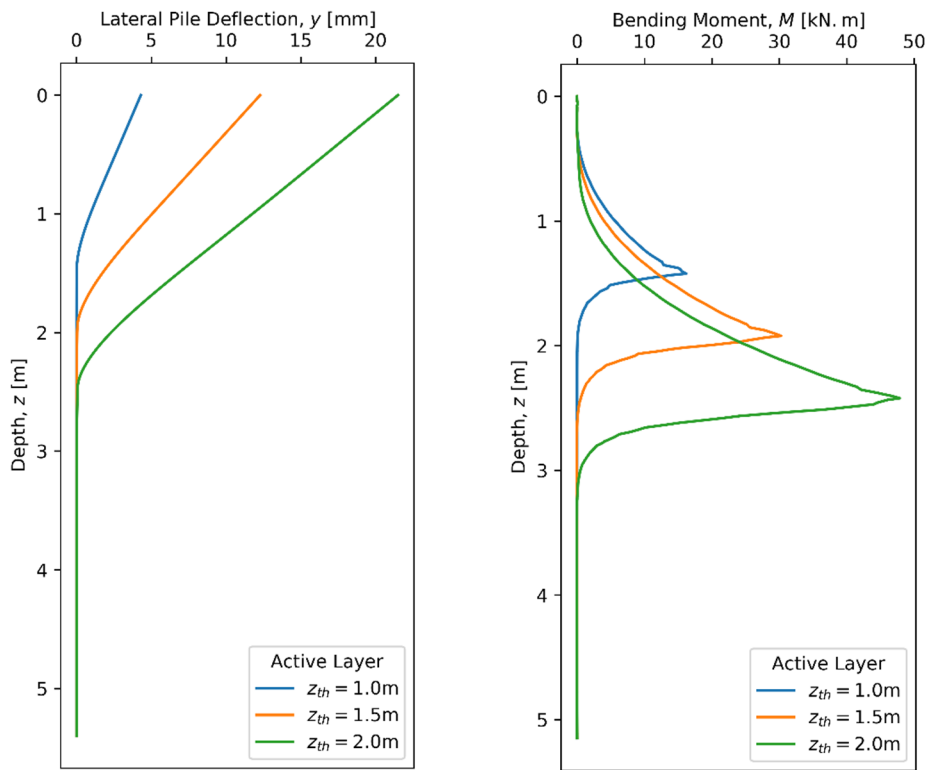
Figure 36: Timber piles - head deflections and bending moments of the toe pile under different active layer thicknesses.
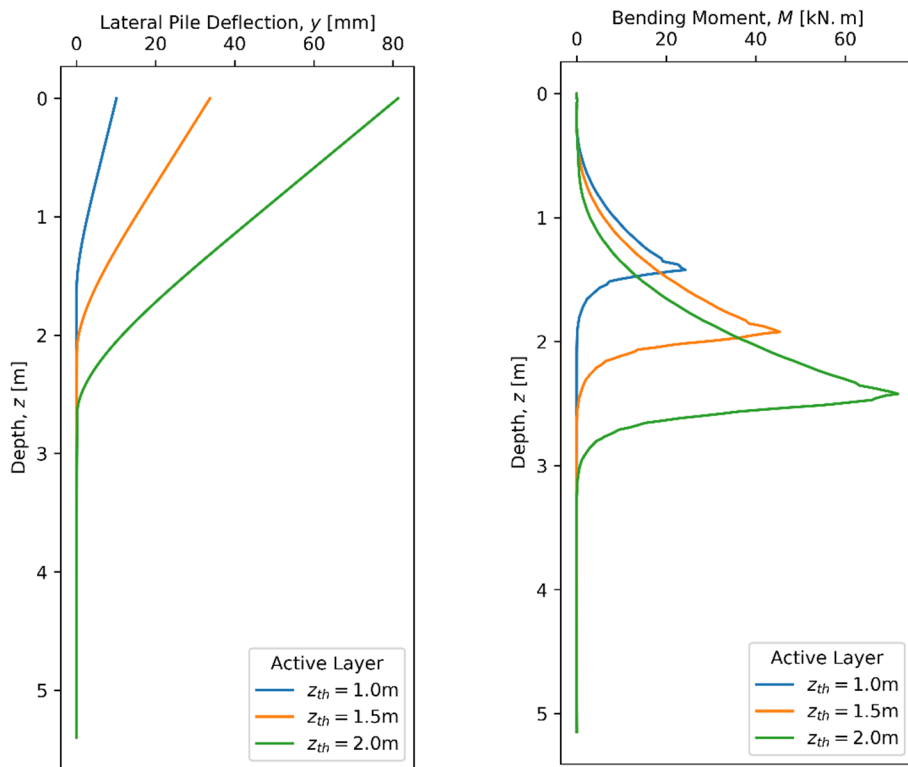

Figure 37: Timber piles - head deflections and bending moments of the mid pile under different active layer thicknesses.

4.6   Bending Capacity of Piles

The failure mode of piles subjected to lateral loading depends on various factors such as the property of the soil, the geometry of the pile and the type of end fixity. Piles may be free-headed or restrained (fixed head) depending on the type of fixity at the top of the pile. Figure 38 shows the common failure modes of free-headed piles, which could occur either through the development of plastic hinges due to bending beyond the yield stress of the material or excessive translational or rotational deformations. Similar failure modes for restrained piles are shown in Figure 39 where the plastic hinges may develop at multiple locations.
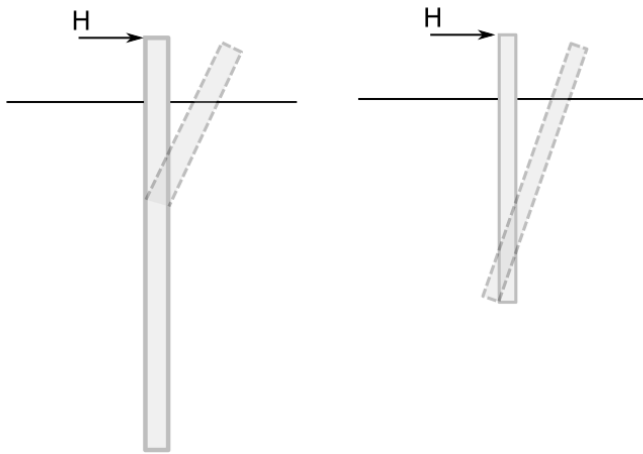

Figure 38: Failure modes for free-headed piles: Long piles – usually through development of plastic hinges due to bending (left) and Short piles – excessive deformation (right); based on [33].
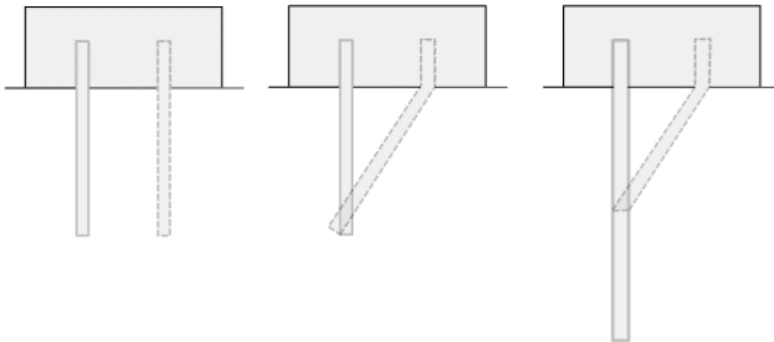
Figure 39: Failure modes for restrained piles through excessive deformation (left) and development of plastic hinges (centre and right), based on [33].

Failure modes with plastic hinges occur when the ultimate flexural strength or yield stress of the material is exceeded. For piles installed in frozen ground with a stiff permafrost layer and a seasonally changing active layer, failure modes with plastic hinges may occur for sufficiently embedded piles. The maximum moment which can be carried by the pile cross-section without exceeding the yield stress must be checked. From beam theory, this maximum yield moment is given by

$$M_y = \frac{\sigma_y I_p}{z} \tag{4.11}$$

where σ_y is the yield stress of the material, I_p is the moment of inertia of the pile and z is the distance from the neutral axis to the extreme tension or compression fibre. For a circular cross-section, the moment of inertia is given by

$$I_p = \frac{\pi d^4}{32} \qquad (4.12)$$

If the yield stress of timber is assumed to be $\sigma_y = 40$ MPa and if a material factor of 0.8 is introduced, the yield moment versus pile diameter plot shown in Figure 40 is obtained. A timber pile with a diameter of 250 mm, as considered in the simulations earlier, yields at a bending moment of around 49 kN m under these conditions.
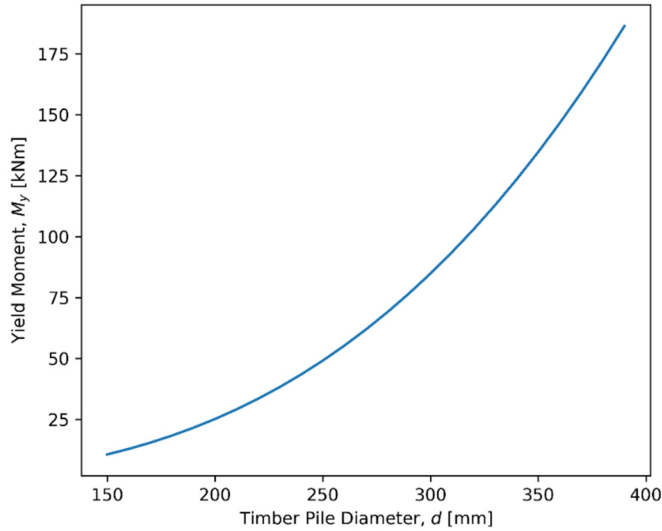
Figure 40: Yield moment versus pile diameter for a round timber pile.

One of the major challenges with timber piles is the problem of aging where structural capacity is lost due to rotting. A simple evaluation of such a capacity loss can be made by assuming that rotting reduces the effective diameter of the pile against bending and shear. If we introduce a factor α (in percentage) to represent such a capacity loss, the yield moment of a rotten pile in terms of the capacity of the original pile may be expressed as

$$M_{y,r} = (1 - \alpha)^3 M_y \qquad (4.13)$$

where $M_{y,r}$ represents the yield moment of the rotten pile. Figure 41 illustrates the capacity reduction of timber piles due to aging according to the assumptions made here.
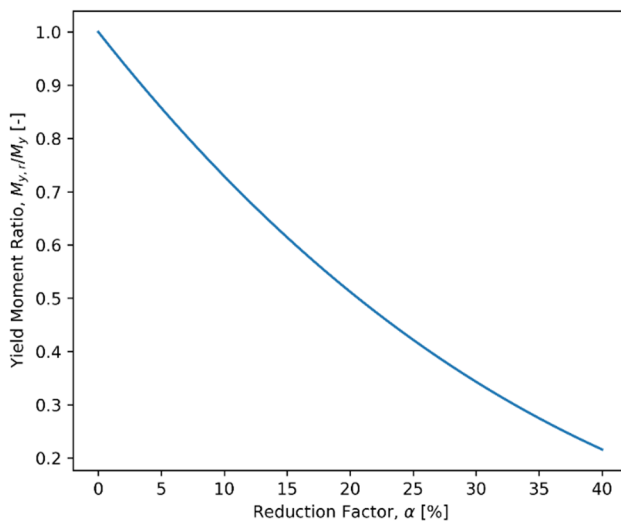
Figure 41: Bending capacity reduction of round timber piles due to aging.

4.7 Summary

The performance of single piles on a slope is investigated by performing various analytical and numerical studies. One of the effects of an increase in active layer thickness on sloping terrains is the risk of solifluction, which is a slow downward movement of soil. The soil movement exerts additional lateral forces on pile foundations, affecting the ultimate capacity of the piles. This is especially significant for building where the effect of solifluction is not considered in the original design. It is observed from the analyses that piles subjected to such additional lateral forces will experience increased deflections and internal forces. The deflections and internal forces increase with increasing slope angles and active layer thicknesses. Piles located in the middle of the slope are observed to experience larger deflections and internal forces than piles located at the toe of the slope. The effect of such increased deflections and internal forces is especially critical for timber piles where the capacity is expected (and shown) to reduce with aging.

5   Case Study on Selected Pile Foundations

5.1   Introduction

This chapter presents a continuation of the study on the effect of climate change on infrastructure in Longyearbyen, on pile foundations on sloping terrains. A general evaluation was performed and reported in the previous chapter. Based on historical temperature trends and future climate projections for Longyearbyen, the changes in ground temperature were analysed. It was shown that, based on RCP8.5 projections, the active layer thicknesses are expected to increase, and the underlying permafrost is expected to get warmer. The effect of these anticipated changes in the ground thermal regime on infrastructure stability were investigated through slope stability analyses and pile capacity modelling. Analytical and numerical calculations were performed in a generic and representative way for the climate and ground conditions in Longyearbyen. The results have shown that the stability of slopes is expected to be affected by the changes in the ground thermal regime and pile foundations are expected to be subjected to increased lateral loads.
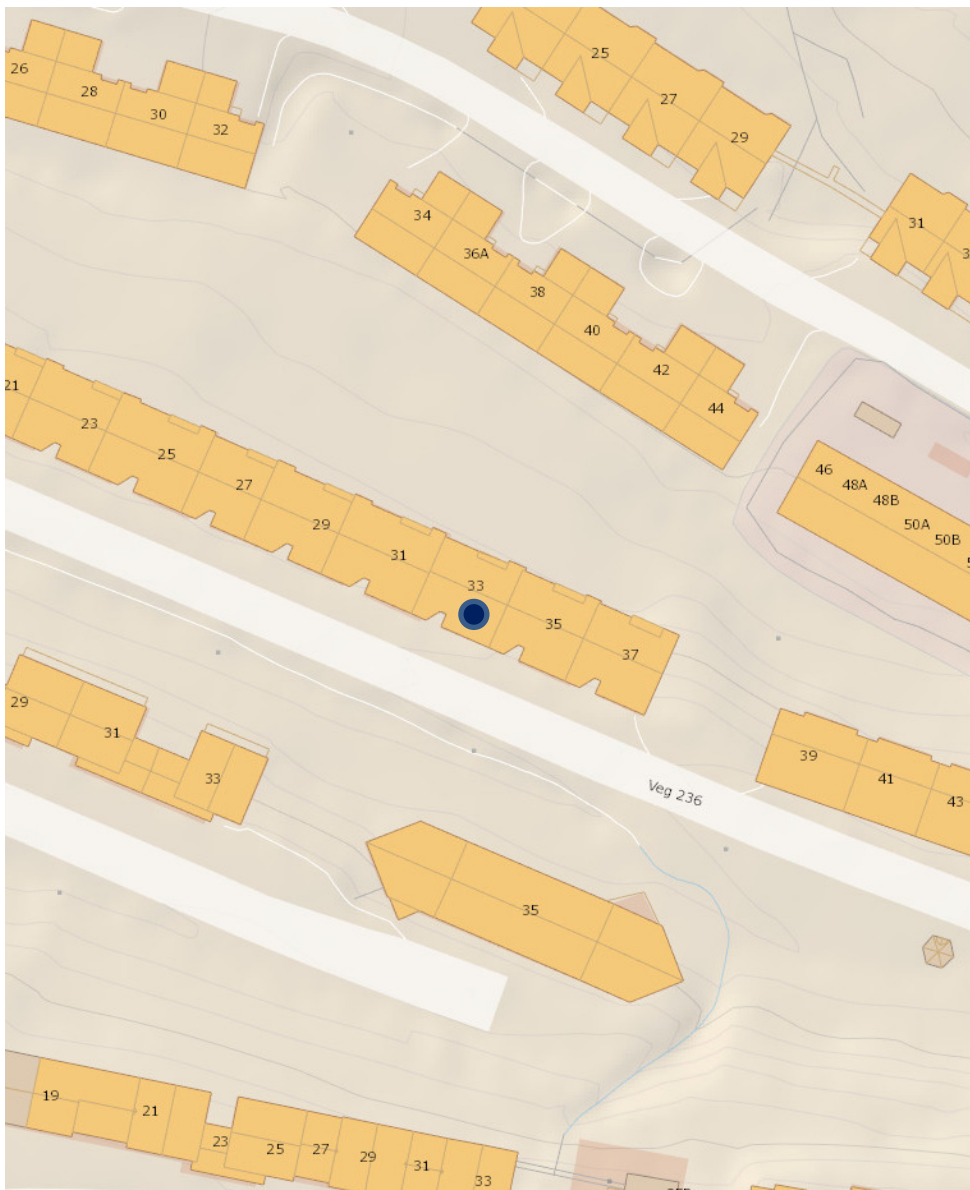

Figure 42: Location of the building selected for the case study; Map: [34].

The objective of the current study is to perform a specific case study for a representative building on a sloping ground and assess the load carrying capacity of the pile foundations under changing ground conditions. The results from the previous study provide inputs required for the specific evaluations. In addition, field and laboratory investigations have been performed in the area; see [35] and [36]. The necessary soil parameters are interpreted based on these investigations and experience for similar ground conditions.

5.2   Building Selected for the Case Study

The building selected for a specific case study is Building 33 on veg 236; see Figure 42. A satellite image of the building and the surrounding area is shown in Figure 43. The selected building is one of a series of attached houses along veg 236. The area features a parking space and a road to the South-West of the building and a sloping ground to the North-East.

Figure 43: Satellite view of the building for the case study and the surrounding area; Picture: [34].

5.3 Site Data

The details of the selected building and the arrangement of the pile foundations is presented in the following section. The ground soil properties required for analyses are presented based on interpretation of the field and laboratory investigations ([37]). The thermal regime of the ground based on ground temperature measurements in the area and thermal analyses from the previous study in the project ([38]) are also summarized here.

5.3.1 Arrangement of Piles

A plan view illustrating the number of piles supporting house 33 and their spacing is shown in Figure 44. The house is supported on 12 timber piles with a spacing of 3.8 m in the direction parallel to the road. The corresponding spacing in the perpendicular direction are 4.4 m and 3.8 m.
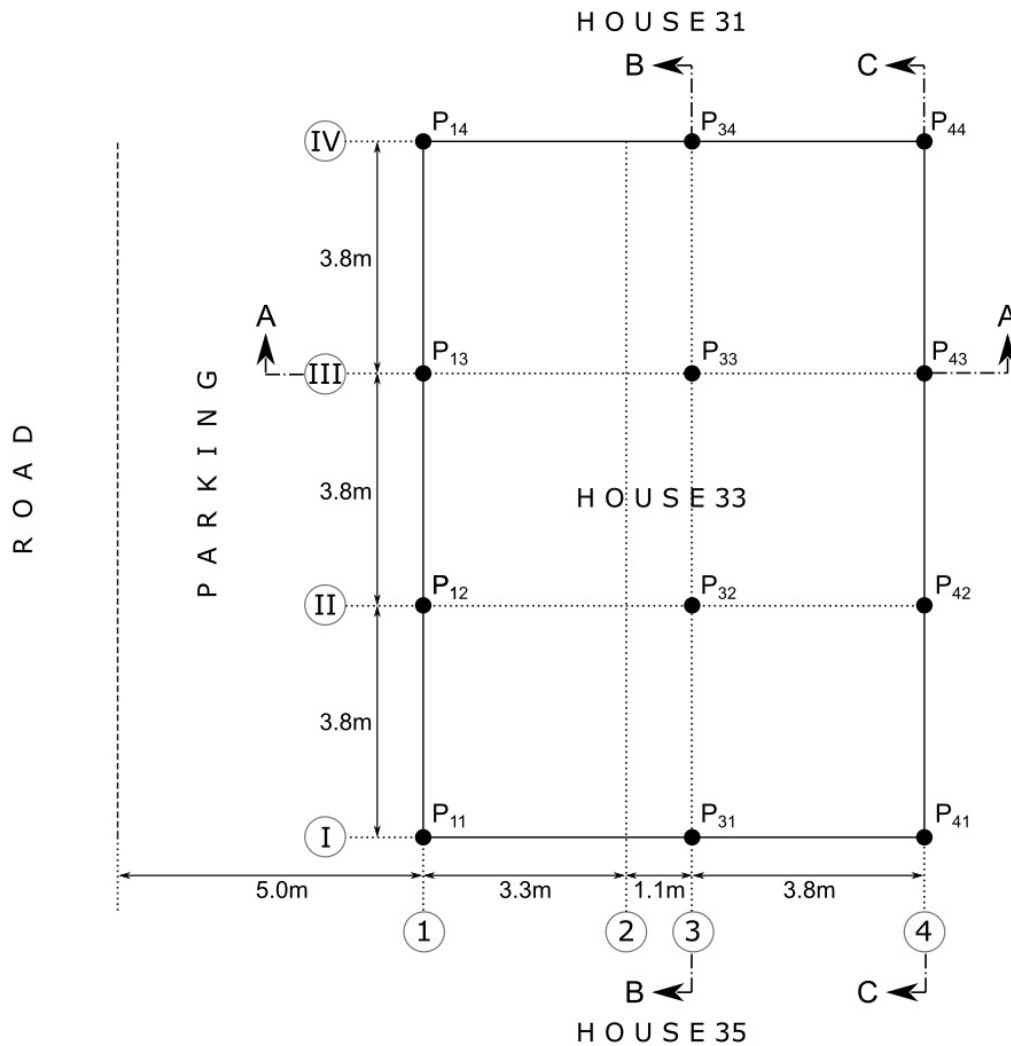
Figure 44: Plan view of house 33 showing the arrangement of the pile foundations.
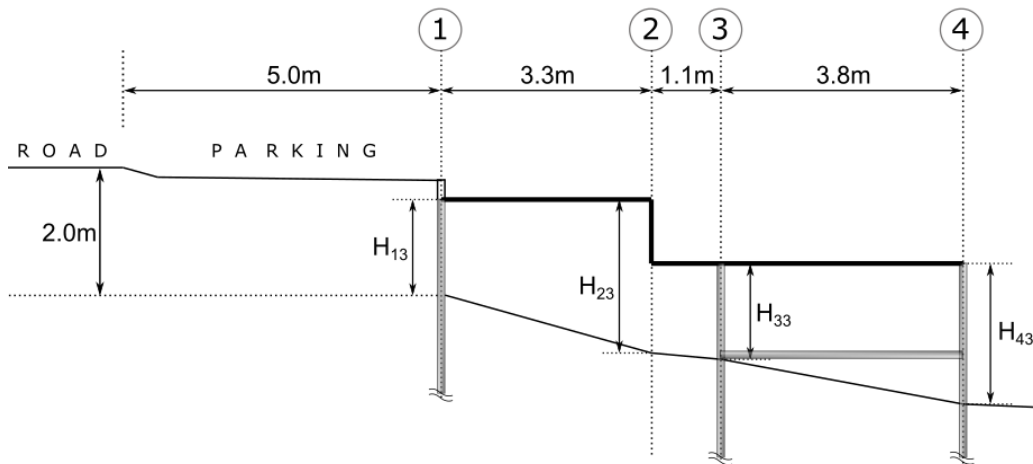
Figure 45: Section A-A.
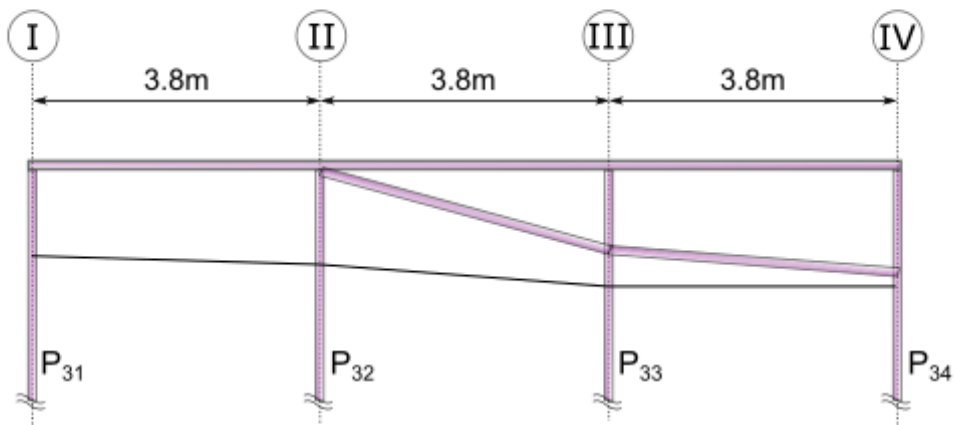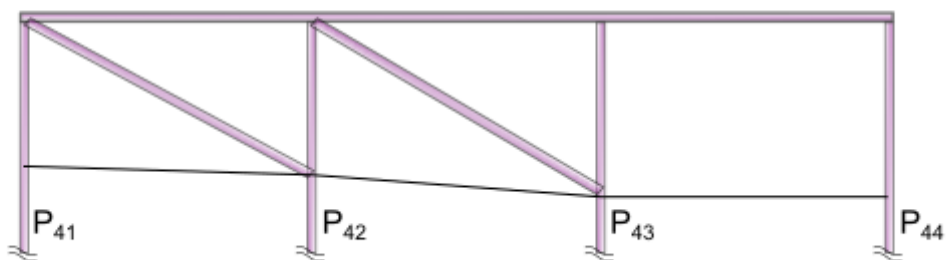
Figure 46: Section B-B and Section C-C.

Cross-section A-A, which shows the pile foundations along the sloping direction of the ground, is shown in Figure 45. Sections B-B and C-C are shown in Figure 46. The pile foundations are elevated from the ground level and there is a number of bracings between some of the piles. The diameter of all piles is ca. 250 mm. The average embedment length of

the piles is ca. 6 m, where there may be slight variations from pile to pile because of ground layer conditions. The piles are assumed to be embedded 1.5 m into the underlying rock bed.

5.3.2 Soil Properties

Two boreholes were drilled close to house 33, where the locations are given in [37]. The depths of the boreholes were 4.6 m and 3.0 m deep. Laboratory testing was performed on soil samples from the boreholes. The average index properties from the laboratory tests are summarized in Table 2.

Table 2: Soil properties from laboratory tests.

Borehole A			
Depth (m)	Water Content (%)	Salinity (%)	Description
0.0 – 0.5	101.5	0.08	Silt or silty clay of low plasticity (OL)
0.5 – 1.0	78.5	-	-
1.0 – 1.5	54.9	-	-
1.5 – 2.0	25.7	0.6	Inorganic silt or clay (ML-CL)
2.0 – 2.5	26.8	-	-
2.5 – 3.0	25.4	-	-
3.0 – 3.5	21.0	0.3	Sand with fines (SM or SC)
3.5 – 4.05	23.0	-	-
4.05 – 4.8	14.0	-	-
Borehole B			
0.0 – 1.0	5.0	-	-
1.0 – 2.0	11.0	-	-
2.0 – 2.65	8.2	0.012	Fine-grained soil

Further index tests on a sample from Borehole A (depth 0.5–1.0 m) resulted in liquid limit, w_L = 38% and plastic limit w_P = 11%, implying a plasticity index of PI = 27%. Based on these index properties, the following soil parameters are assumed for the active layer; Table 3. The properties for permafrost are estimated based on these assumed parameters and the temperature of the permafrost.

Table 3: Soil parameters assumed for analysis.

Parameter	Lower Bound (LB)	Upper Bound (UB)
Unit weight, γ (kN/m^3)	15.0	19.0
Friction angle, ϕ (deg)	25.0	30.0
Cohesion, c (kPa)	10.0	30.0

Ways of estimating drained strength parameters based on index properties such as plasticity index may be referred from [39].

5.3.3 Ground Temperature Data

Ground temperature at the site was monitored using a thermistor string. The first plot in Figure 47 shows the temperature reading on November 1st 2017. Ground thermal analyses were performed based on projected air temperature data and the expected temperature profiles for selected years are shown in the second plot in

Figure 47. The profiles are shown for the last dates of the thawing season for each year, before the active layer starts freezing again. The active layer thicknesses are expected to increase as a result of climate change. Some of the ground temperature measurements, for example the one shown here, indicate an active layer thickness of about 2 m. The thermal analyses show active layer thicknesses from about 1 m to ca. 2 m based on projections. Such differences are expected to result from uncertainty in soil parameters and variation of soil properties in Longyearbyen. For pile capacity analyses, a range of active layer thicknesses will be considered to account for current conditions and future projections.
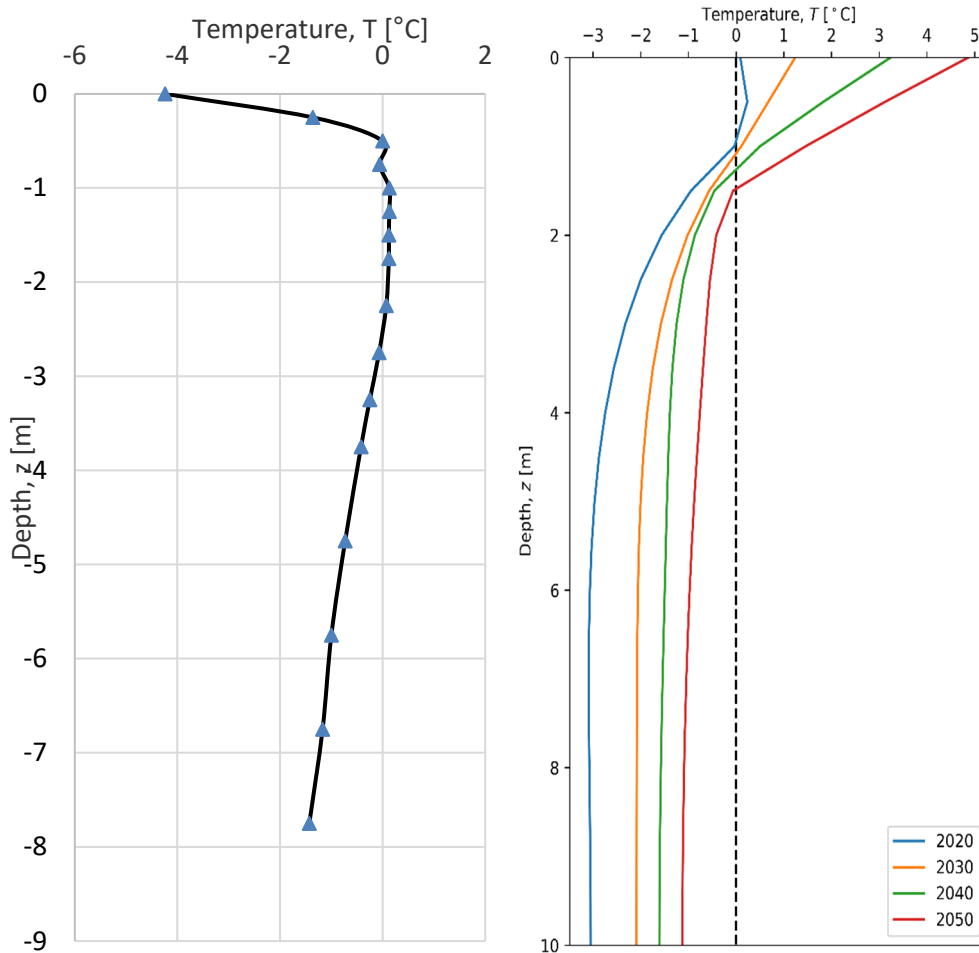
Figure 47: Left - Ground temperature measurements on November 1, 2017 and Right – Ground temperatures estimated based on projected air temperature data; the temperature profiles are shown for dates corresponding to the end of the thawing season for each year.

5.4 Pile Response Analyses

5.4.1 Loads on Piles

The axial loads acting on the pile are estimated based on standard calculation procedure considering dead and live loads. The calculations are performed according to the SINTEF Byggforsk Anvisninger (Codes of Practise) [40] and [41], which present estimation of line loads on foundation beams for a two-storey building considering the self-weight of the building and other loads. The axial loads on each pile are estimated by assuming an equal distribution of the load among the piles.

As the building is located on a sloping terrain, the piles will be subjected to lateral loads as a result of earth pressure. These earth pressure may be a result of slope processes in the active layer (for example due to solifluction, which includes creep of permafrost beneath the active layer) and from direct loads at the crest (from parking and road). The lateral loads from these sources are difficult to estimate accurately. The approach followed here is to rely on the numerical simulation performed previously by initiating slope processes with various active layer thicknesses, [38]. The pressure on the pile for these different active layer thicknesses are used as a basis and converted to resultant systems at the pile top.

5.4.2 Representative Model

Borehole data at the site shows that the bedrock is located at ca. 4.5 m below ground surface. The piles are estimated to be embedded at least 1.5 m into the bedrock, which may be characterized as a soft/brittle rock.
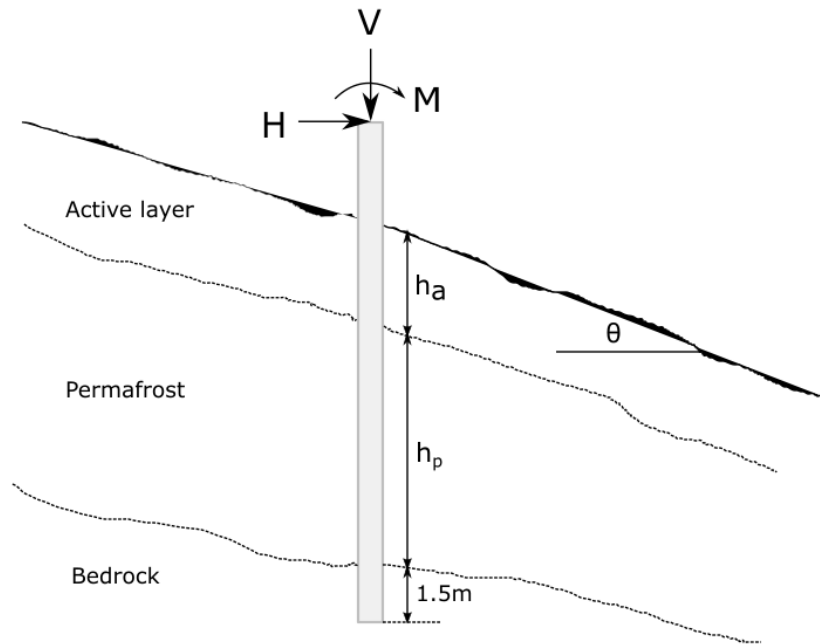

Figure 48: Representative model for pile response analysis.

The model shown in Figure 48 is used as a basic template for various analyses. Different variation in the active layer thickness h_a and the permafrost thickness h_p are considered. Different combinations of axial, lateral and bending moment loads (V, H and M) are also considered. In particular, the lateral load is expected to be dependent on the value of the active layer thickness for lateral loading which is initiated by slope processes such as solifluction. The analyses combinations considered are summarized in Table 4.

Table 4: Active layer thickness and load combinations.

Active Layer, h_a (m)	Axial Load, V (kN)	Lateral Load, H (kN)
1.5	50	20
	100	25
	150	30
2.5	50	40
	100	45
	150	50
3.5	50	60
	100	65
	150	70

In the analyses performed here, a resultant loading system at the top of the pile is assumed. The actual lateral loads due to slope processes are applied as a distributed load along the length of the pile embedded in the active layer. These lateral loads are converted to resultant forces and moments at the top of the pile through simple equilibrium considerations. Some of the piles have bracing supports and the expected support contributions are indirectly considered in the resultant system reducing the lateral loads and bending moments. The pile stick-up length above the ground varies throughout the building, and an average of ca. 1.0 m is assumed. Other variations are compensated by considering various load combinations.

5.4.3 Methodology for Analysis

The capacity of the piles for the selected building is calculated analytically based on *p-y* curves. The analytical equations applied here as presented in Section 4.3.

5.4.4 Results

Figure 49 presents the pile head deflection, bending moment and shear force for a pile subjected to an axial load of 50 kN and lateral loads ranging from 20 to 60 kN. The range of lateral loads correspond to active layer thicknesses of 1.5, 2.5 and 3.5 m which consider current and anticipated changes in the ground thermal regime. These combinations result in pile head deflections from around 20 mm for the lowest lateral load to more than 60 mm for the highest.
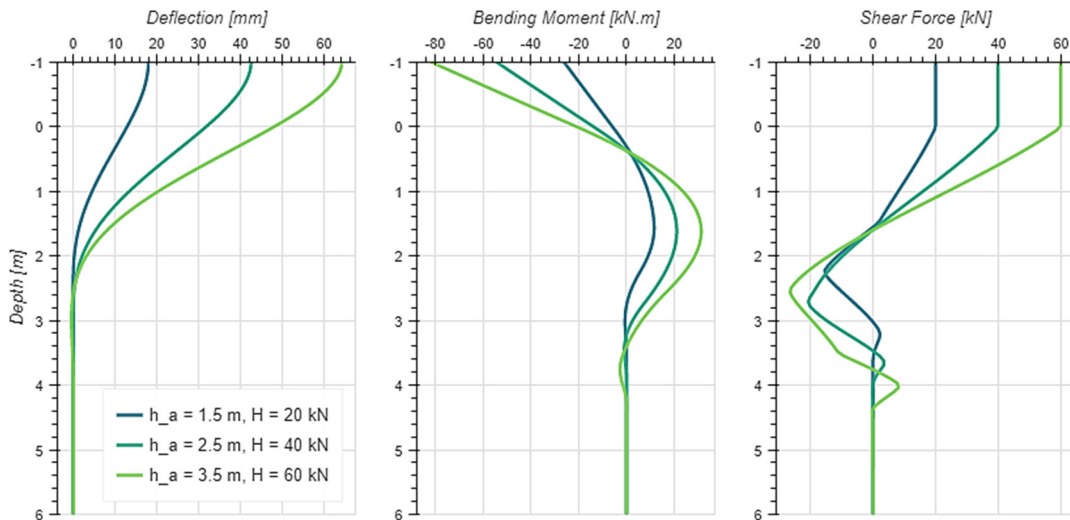
Figure 49: Pile deflections and internal forces; axial load V = 50 kN.

Figure 50: Pile deflections and internal forces; axial load V = 100 kN.

Similar results for an axial load of 100 kN and the same range of active layer thicknesses are shown in Figure 50. Slightly increased lateral loads from 25 to 65 kN are applied at the pile heads, which are estimated based on equilibrium resultant systems. Increased deflections and internal forces are observed, as expected.
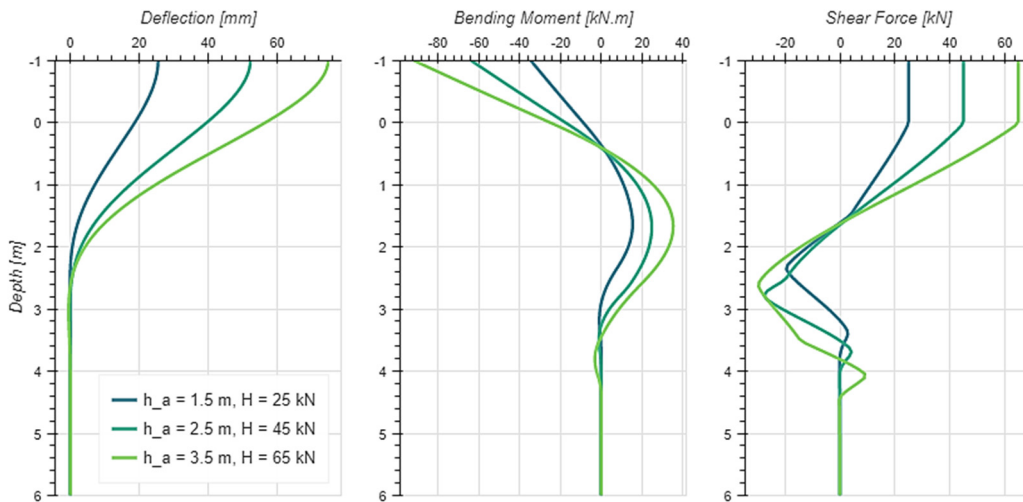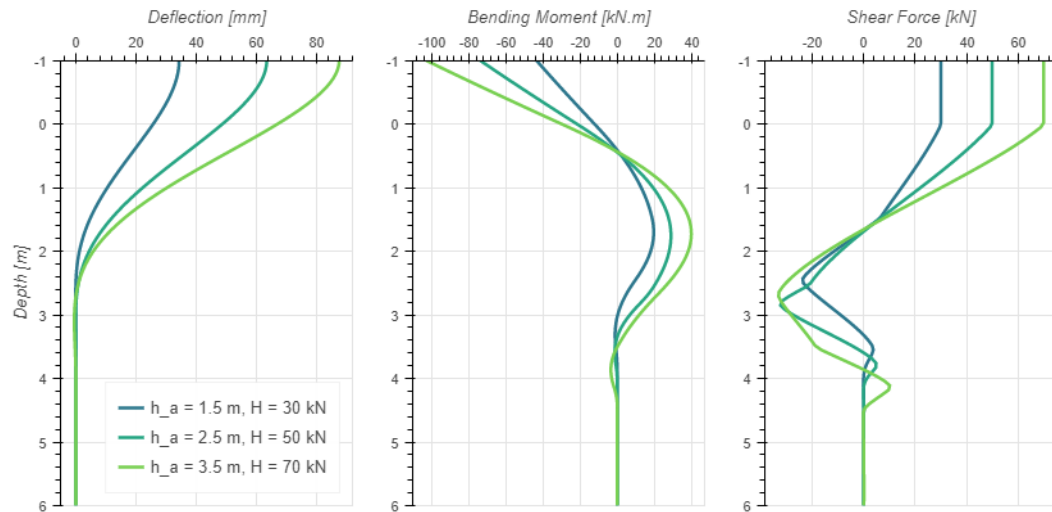
Figure 51: Pile deflections and internal forces; axial load V = 150 kN.

5.5 Summary

The effects of increased lateral loads, as a result of thawing and warming permafrost, on the pile foundations of a selected building in Longyearbyen located on a slope are investigated through numerical analyses. A range of active layer thicknesses are considered in the analyses taking current and projected scenarios into account. The axial loads on the piles are estimated based on standard methods for residential buildings, and variations are considered to account for uncertainties. The lateral loads on the piles are assumed to mainly originate from slope movements (such as solifluction) and loads transferred from crest of the slope through earth pressure. The finite element simulations performed in a general way are used a basis to estimate the earth pressures on the piles and the loads are converted to an equivalent resultant system at the pile head for simplicity of the analyses. Variations in the lateral loads are considered corresponding to the range of active layer thicknesses. Analyses based on p-y curves are performed for the different active layer thicknesses and loads considered. The results are presented in terms of pile head deflections, bending moments and shear forces. It is shown that the pile head deflections are expected to increase as the active layer thicknesses increase. A similar trend of increase is observed in the internal forces generated in the piles.

References

1. ACIA, *Arctic Climate Impact Assessment.* Cambridge University Press, 2005: p. 1042.
2. Nordli, O., et al., *Long-term temperature trends and variability on Spitsbergen: the extended Svalbard Airport temperature series, 1898-2012.* Polar Research, 2014. **33**.
3. Hanssen-Bauer, I. and E.J. Forland, *Long-term trends in precipitation and temperature in the Norwegian Arctic: can they be explained by changes in atmospheric circulation patterns?* Climate Research, 1998. **10**(2): p. 143-153.
4. Forland, E.J., et al., *Temperature and Precipitation Development at Svalbard 1900-2100.* Advances in Meteorology, 2011.
5. Benestad, R.E., et al., *Climate change and projections for the Barents region: what is expected to change and what will stay the same?* Environmental Research Letters, 2016. **11**(5).
6. TIME. 2016; Available from: https://apple.news/AuFeGpgeeSD6_7WEtR_NeJQ.
7. Esch, D.C., Osterkamp, T.E., *Climate warming concerns for Alaska.* Journal of Cold Regions Engineering, 1990. **4**(1): p. 6-14.
8. Instanes, A., *Climate change and possible impact on Arctic infrastructure.* Permafrost, Vols 1 and 2, 2003: p. 461-466.
9. Kokelj, S.V., et al., *Increased precipitation drives mega slump development and destabilization of ice-rich permafrost terrain, northwestern Canada (vol 129, pg 56, pg 2015).* Global and Planetary Change, 2015. **135**: p. 207-207.
10. Larsen, M., *Personal communication*. 2016.
11. Sinitsyn, A., *Impact of changing climate on infrastructure in Longyearbyen: Stability of foundations on slope terrain - case study.* Project Application, 2016.
12. Sinitsyn, A., *Impact of changing climate on infrastructure in Longyearbyen: Stability of foundations on slope terrain - case study.* Presentation for Project Kick-off Meeting., 2017.
13. Andersland, O.B., B. Ladanyi, and O.B. Andersland, *Frozen ground engineering*. 2nd ed. 2004, Hoboken, NJ, Reston, Va.: Wiley. xii, 363 p.
14. Zhang, T., T.E. Osterkamp, and K. Stamnes, *Effects of climate on the active layer and permafrost on the north slope of Alaska, USA.* Permafrost and Periglacial Processes, 1997. **8**(1): p. 45-67.
15. Carpentier, M., *Climate and Slope Influence on the Lateral Loading of Piles in the Permafrost of Svalbard.* MSc Thesis, UNIS and NTNU, 2017.
16. NPI. Available from: http://toposvalbard.npolar.no/.
17. Bauer, J., O. Reul, and H.G. Kempfert, *Lateral pressure on piles due to horizontal soil movement.* International Journal of Physical Modelling in Geotechnics, 2016. **16**(4): p. 173-184.
18. Chow, Y.K., *Analysis of piles used for slope stabilization.* International Journal for Numerical and Analytical Methods in Geomechanics, 1996. **20**(9): p. 635-646.
19. Georgiadis, K. and M. Georgiadis, *Development of p-y curves for undrained response of piles near slopes.* Computers and Geotechnics, 2012. **40**: p. 53-61.
20. Gu, Q., Z.H. Yang, and Y. Peng, *Parameters affecting laterally loaded piles in frozen soils by an efficient sensitivity analysis method.* Cold Regions Science and Technology, 2016. **121**: p. 42-51.
21. Harris, C., M.C.R. Davies, and J.P. Coutard, *An experimental design for laboratory simulation of periglacial solifluction processes.* Earth Surface Processes and Landforms, 1996. **21**(1): p. 67-75.
22. Jeong, S., et al., *Uncoupled analysis of stabilizing piles in weathered slopes.* Computers and Geotechnics, 2003. **30**(8): p. 671-682.
23. Liyanapathirana, D.S. and H.G. Poulos, *Analysis of pile behaviour in liquefying sloping ground.* Computers and Geotechnics, 2010. **37**(1-2): p. 115-124.
24. Martin, G.R. and C.Y. Chen, *Response of piles due to lateral slope movement.* Computers & Structures, 2005. **83**(8-9): p. 588-598.

25. Yang, Z.H., et al., *Performance and Design of Laterally Loaded Piles in Frozen Ground.* Journal of Geotechnical and Geoenvironmental Engineering, 2017. **143**(5).

26. Harris, S.A., French, H.M., Heginbottom, J.A., Johnston, G.H., Ladanyi, B., Sego, D.C, van Everdigen, R.O., *Glossary of permafrost and related ground-ice terms.* Associate Committee on Geotechnical Research, National Research Council of Canada, Ottawa, 1988. **156**.

27. Tart, R.G., *Heave and solifluction on slopes.* Permafrost, Vols 1 and 2, 2003: p. 1135-1140.

28. Crowther, G.S., *Lateral Pile Analysis Frozen Soil Strength Criteria.* Journal of Cold Regions Engineering, 2015. **29**(2).

29. Tsegaye, A.B., Guegan, E., Nordal, S., *Modeling the strength of frozen saturated soil.* 2015, Norwegian University of Science and Technology: Trondheim, Norway.

30. Reese, L.C., W.M. Isenhower, and S.-T. Wang, *Analysis and design of shallow and deep foundations.* 2006, Hoboken, N.J.: John Wiley. xxxiii, 574 p.

31. Sluis, J.J.M., F. Besseling, and P.H.H. Stuurwold, *Modelling of a pile row in a 2D plane strain FE-analysis.* Numerical Methods in Geotechnical Engineering, Vol 1, 2014: p. 277-282.

32. Ashour, M. and H. Ardalan, *Analysis of pile stabilized slopes based on soil-pile interaction.* Computers and Geotechnics, 2012. **39**: p. 85-97.

33. Broms, B.B., *Lateral resistance of piles in cohesive soils.* Journal of the Soil Mechanics and Foundations Division, 1964. **90**(2): p. 27-64.

34. Norwegian Polar Institute. *TopoSvalabrd.* 2017; Available from: http://toposvalbard.npolar.no/.

35. Christensen, S.O., *Impact of changing climate on infrastructure in Longyearbyen: stability of foundations on slope terrain – Case study. Field report – geotechnical investigations.* 2017, SINTEF: Trondheim.

36. Carpentier, M., *Climate and Slope Influence on the Lateral Loading of Piles in the Permafrost of Svalbard.* 2017, Norwegian University of Science and Technology (NTNU), The University Centre in Svalbard (UNIS). p. 48.

37. Sinitsyn, A., *Impact of changing climate on infrastructure in Longyearbyen: stability of foundations on slope terrain – case study. Field and Laboratory Report 2018 – Geotechnical Investigations.* 2019, SINTEF: Trondheim.

38. Bekele, Y. and A. Sinitsyn, *Impact of changing climate on infrastructure in Longyearbyen: stability of foundations on slope terrain – Case study. Project Report 2017.* 2017, SINTEF: Trondheim.

39. Sorensen, K. and N. Okkels. *Correlation between drained shear strength and plasticity index of undisturbed overconsolidated clays.* in *Proceedings of the 18th International Conference on Soil Mechanics and Geotechnical Engineering, Paris.* 2013.

40. Byggforskserien 471.031, *Egenlaster for bygningsmaterialer, byggevarer og bygningsdeler.* 2013, SINTEF Byggforsk: Oslo.

41. Byggforskserien 521.111, *Golv på grunnen med ringmur. Utførelse.* 2012, SINTEF Byggforsk: Oslo.

Impact of Climate Change on Infrastructure in Longyearbyen

CASE STUDY OF PILE FOUNDATIONS ON SLOPING TERRAINS

This report presents findings from studies in the project entitled "Impact of Changing Climate on Infrastructure in Longyearbyen: Stability of Foundations on Slope Terrain – Case Study" carried out at SINTEF. The initiative targeted planning in Longyearbyen, Svalbard under conditions of climate change.

The particular focus of the study are slopes and buildings supported on sloping terrains in Longyearbyen. Changes in ground temperature are investigated based on existing temperature data and forecasts. The ground thermal regime is then used to evaluate the stability of representative slopes in the study area. The capacity of single piles on a slope is also investigated by considering various factors such as slope angle, location of pile on slope, pile material and geometry.

In general, the study highlights the importance of assessing the effect of climate change on existing infrastructure to ensure safety and serviceability. The knowledge gained from the study also highlights the necessity of the consideration of climate change in the design of new infrastructure to be built in affected areas.

SINTEF